Suppl. Figure 1

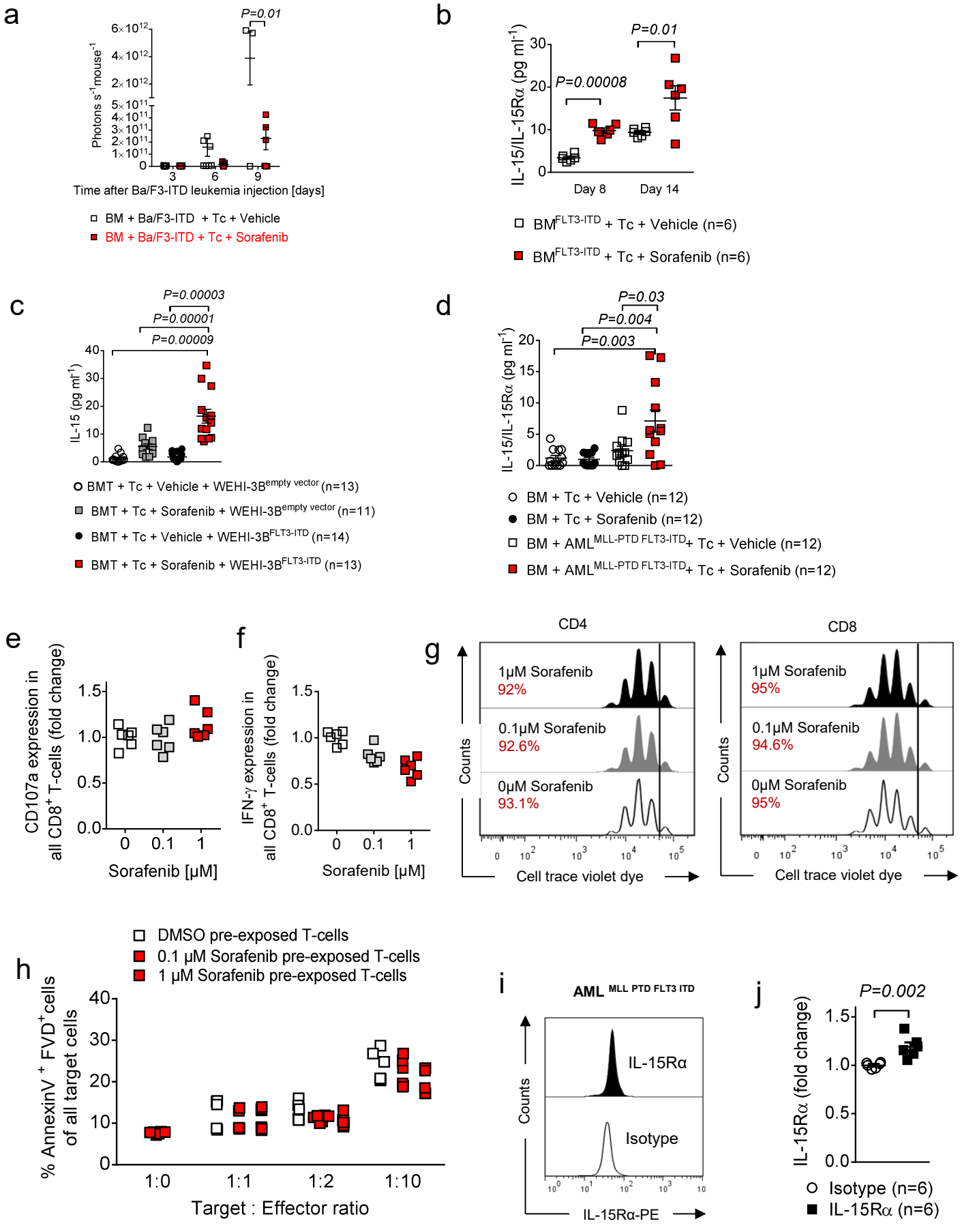

Suppl. Figure 2

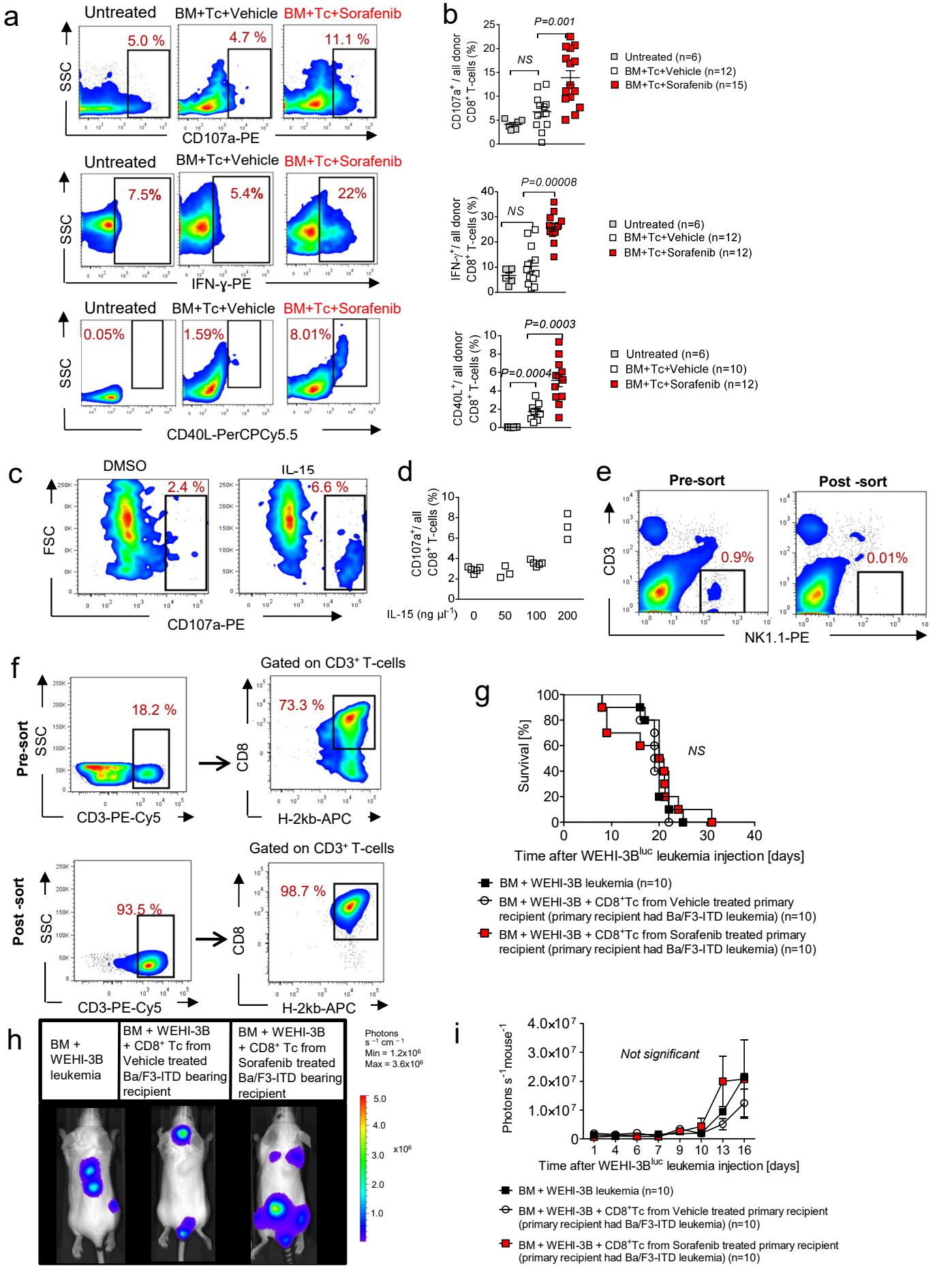

Suppl. Figure 3

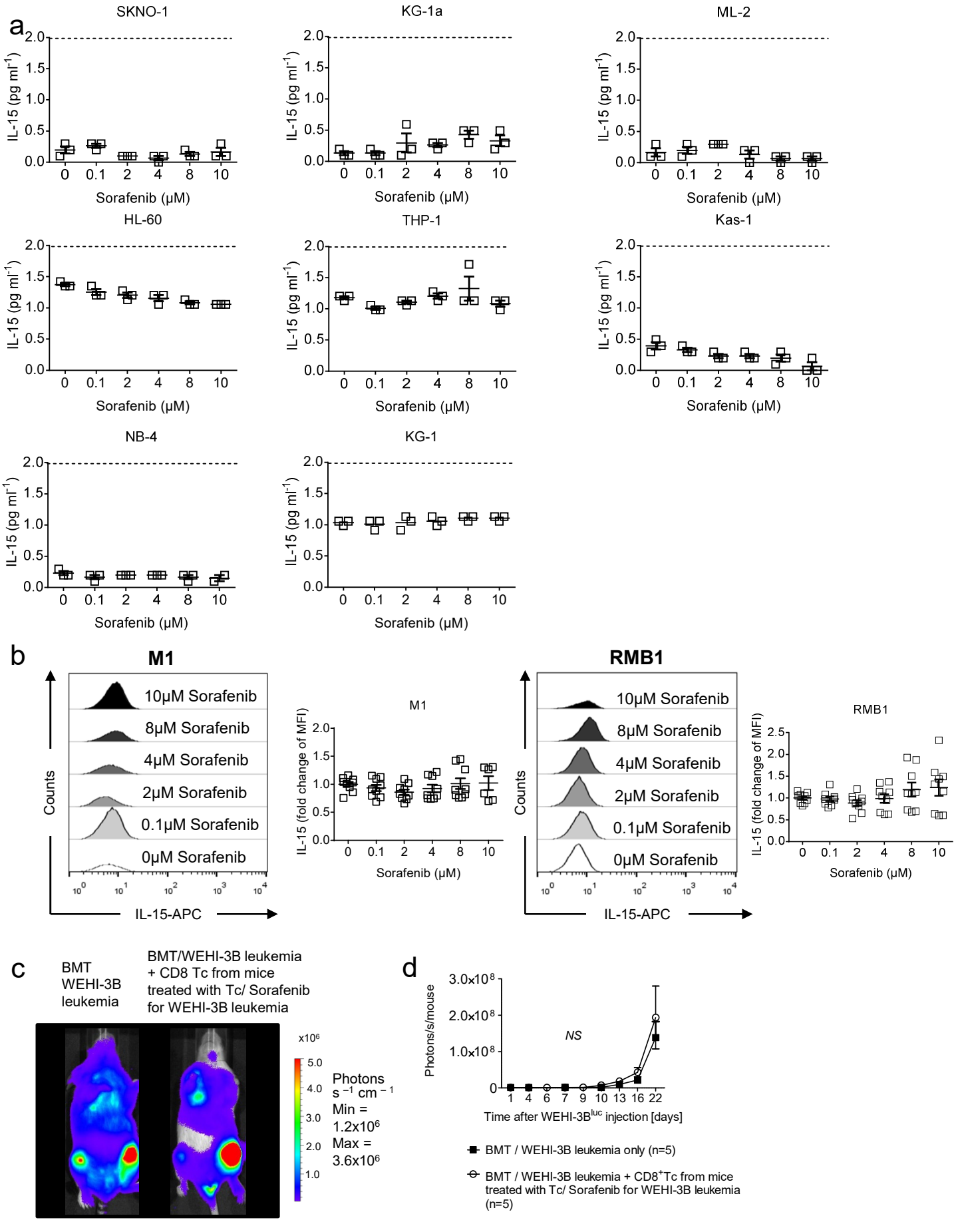

Suppl. Figure 4

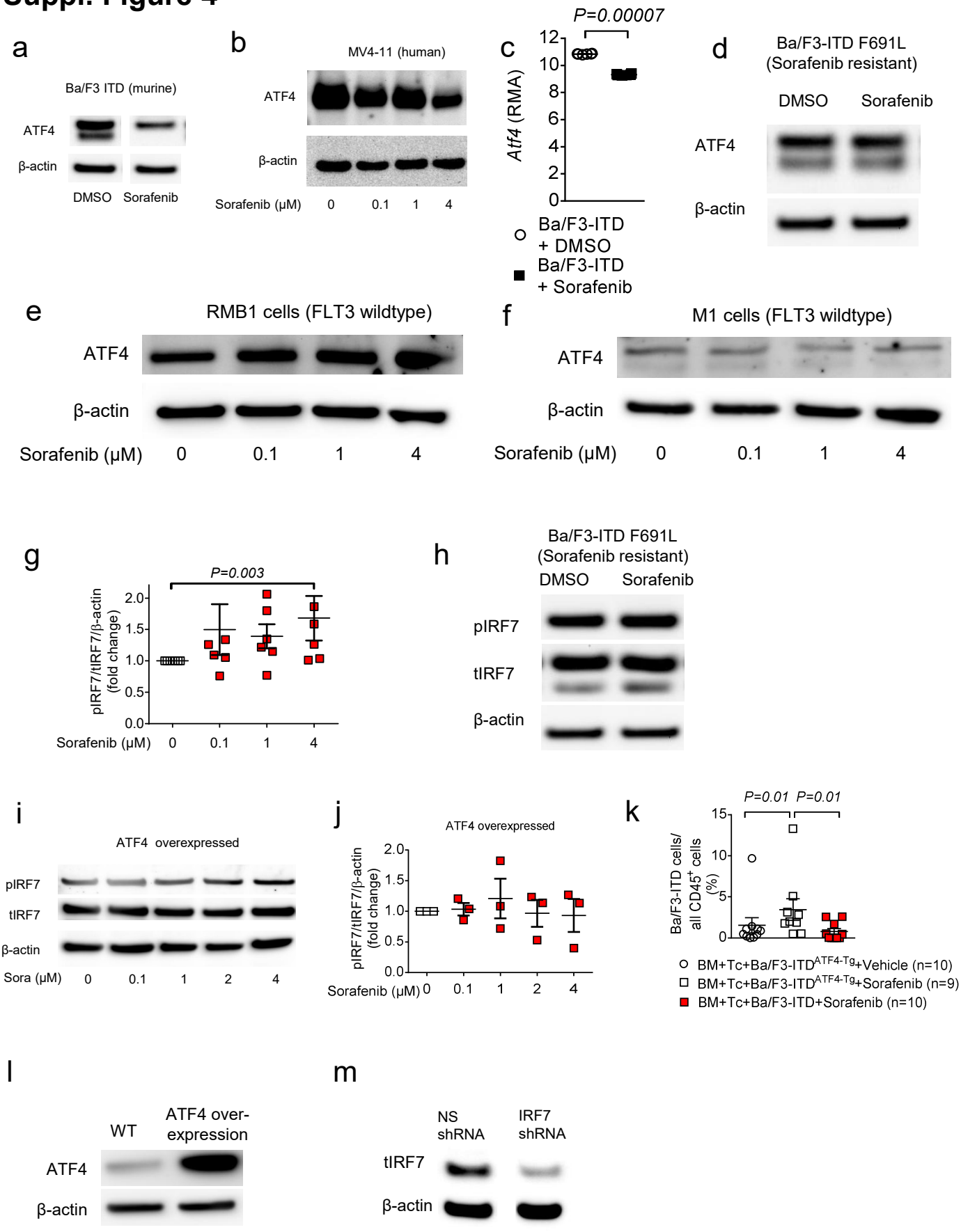

Suppl. Figure 5

a

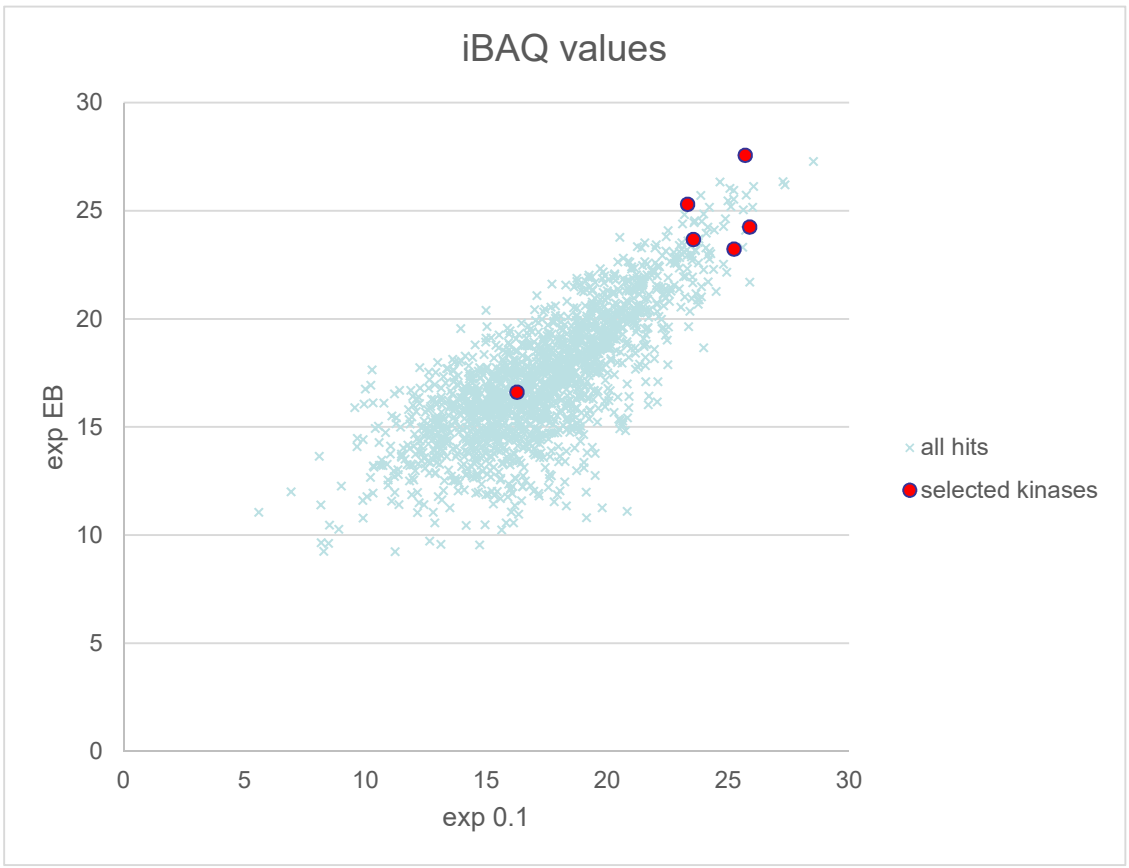

Suppl. Figure 6

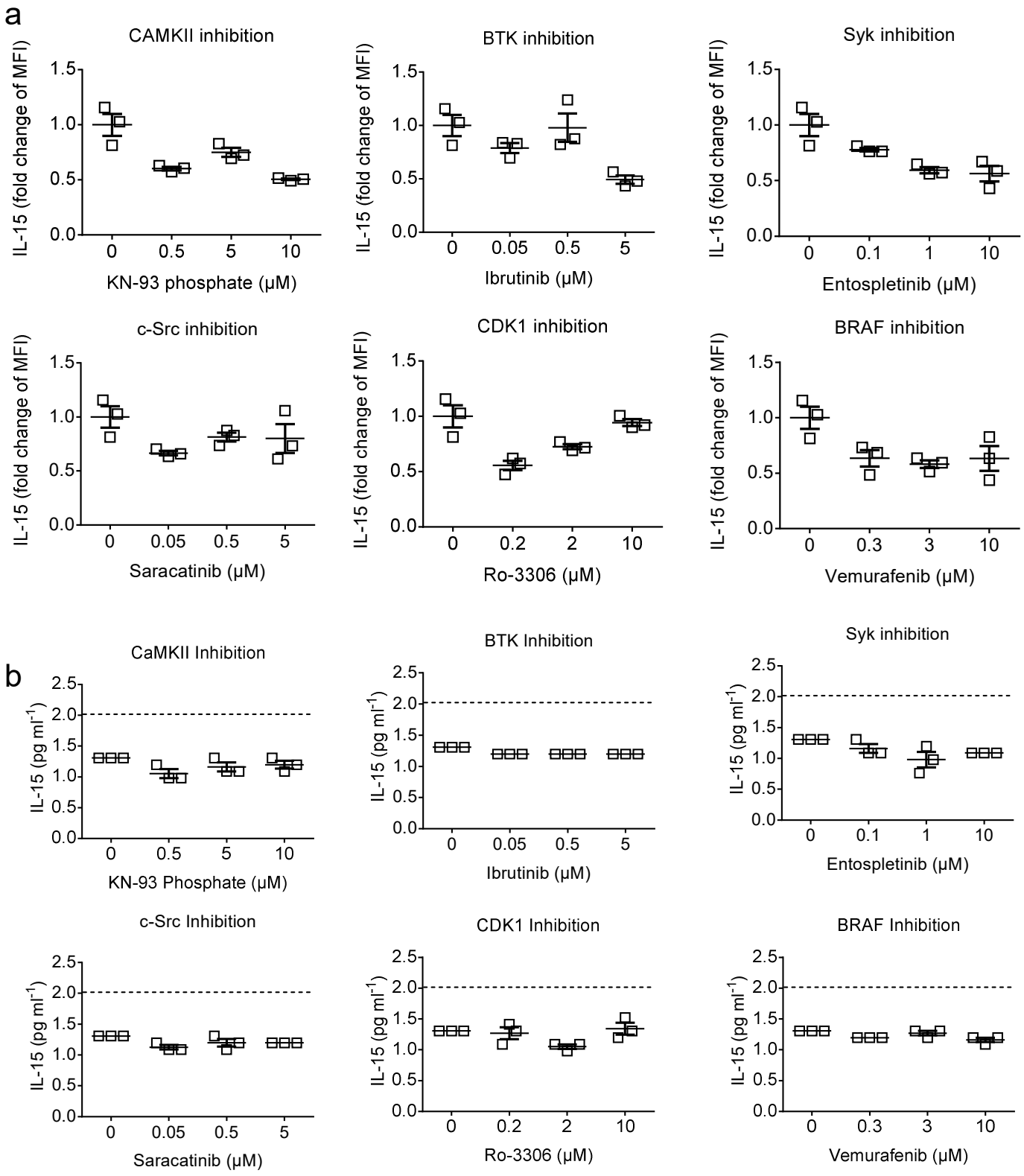

Suppl. Figure 7

a

Kinase	EC_{50}	K_d^{app}	R2
PRKAB2	612.8	54.8	0.75
MAP3K5	632.5	120.9	0.76
FLT3	684.4	466.3	0.86
ZAK	712.5	712.5	0.89
MAP3K1	2530	1255.9	0.83
CDK16	1602	1602	0.81

Suppl. Figure 8

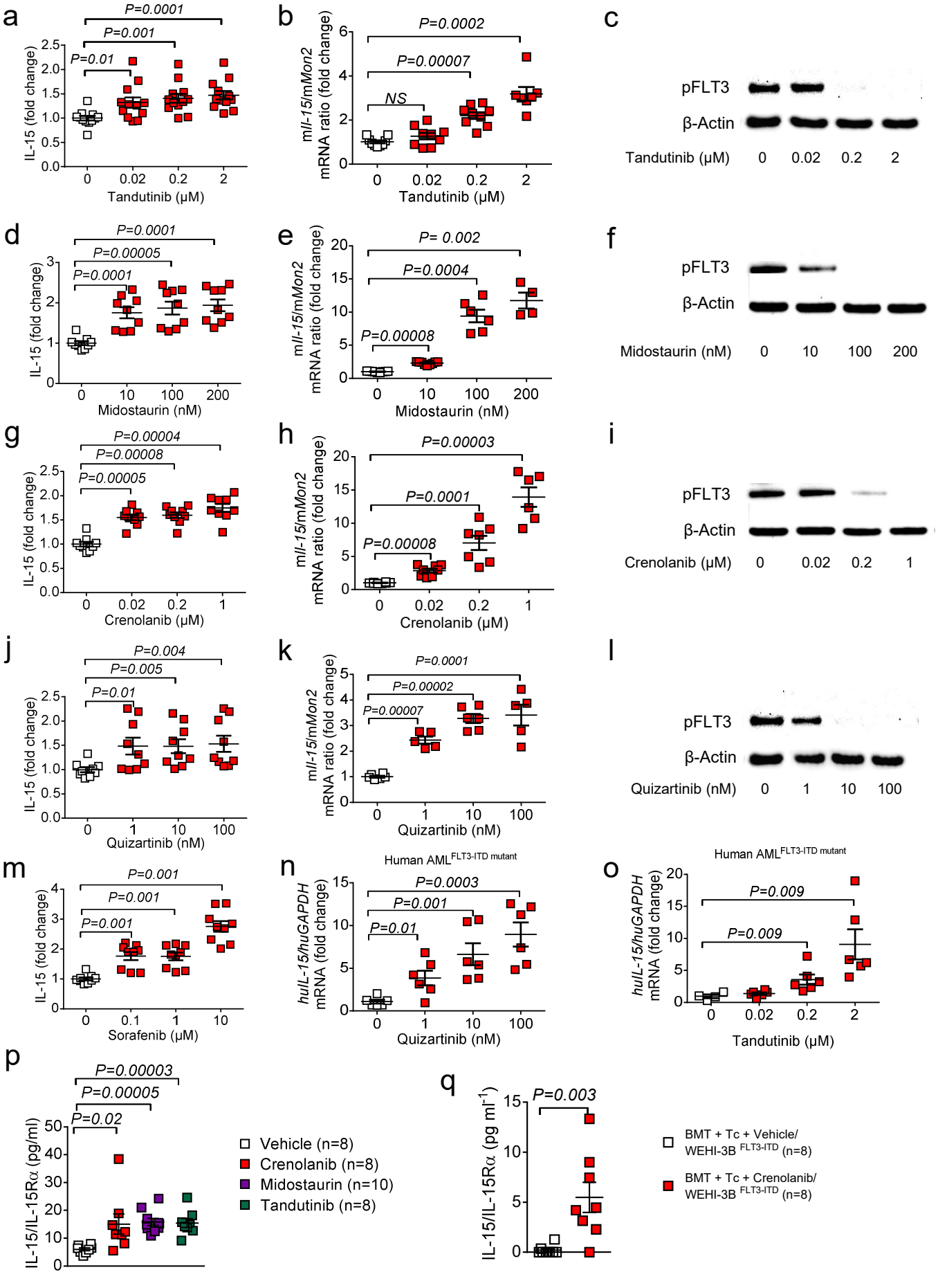

Suppl. Figure 9

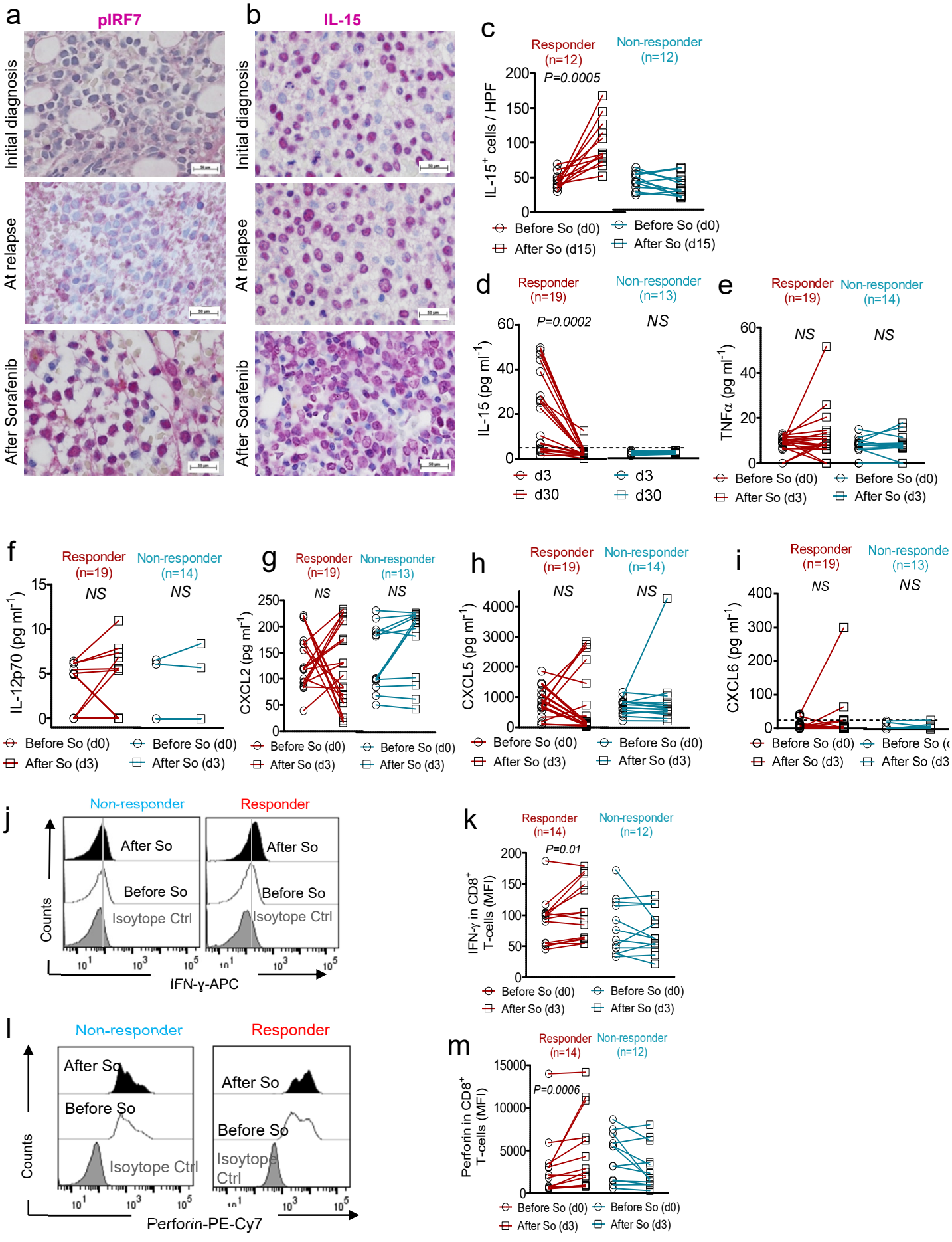

Suppl. Figure 10

a Exonic somatic mutations

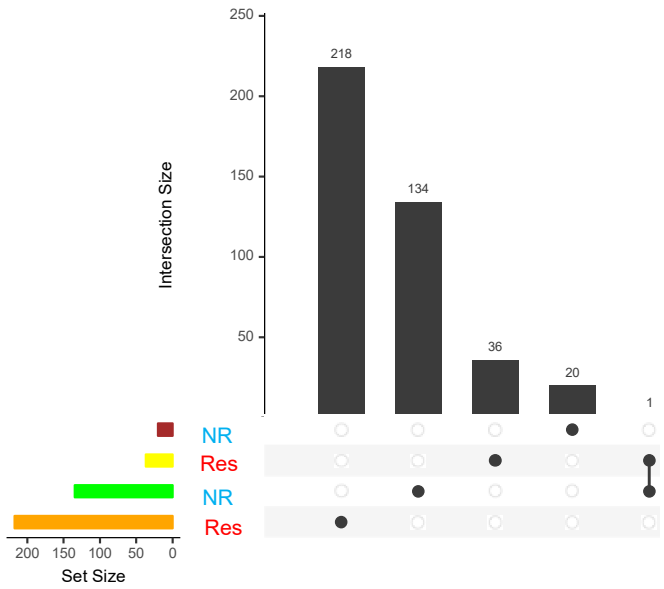

b Intronic/Exonic somatic mutations

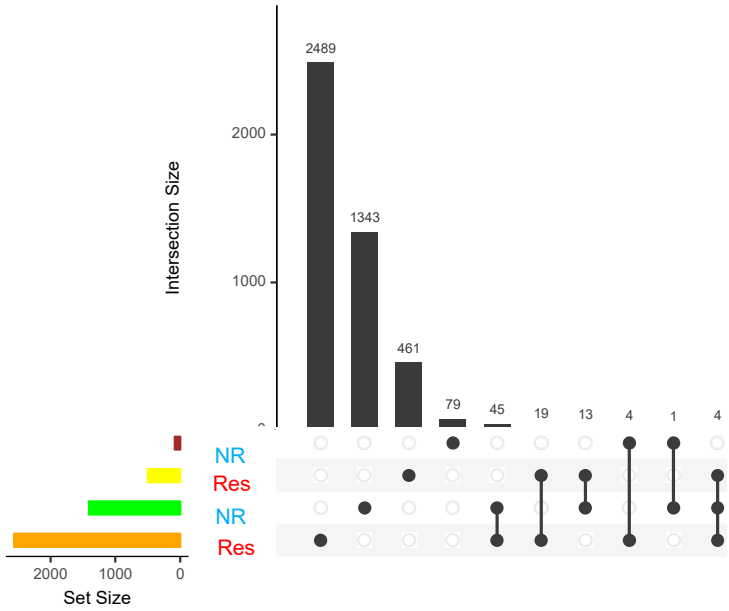

c

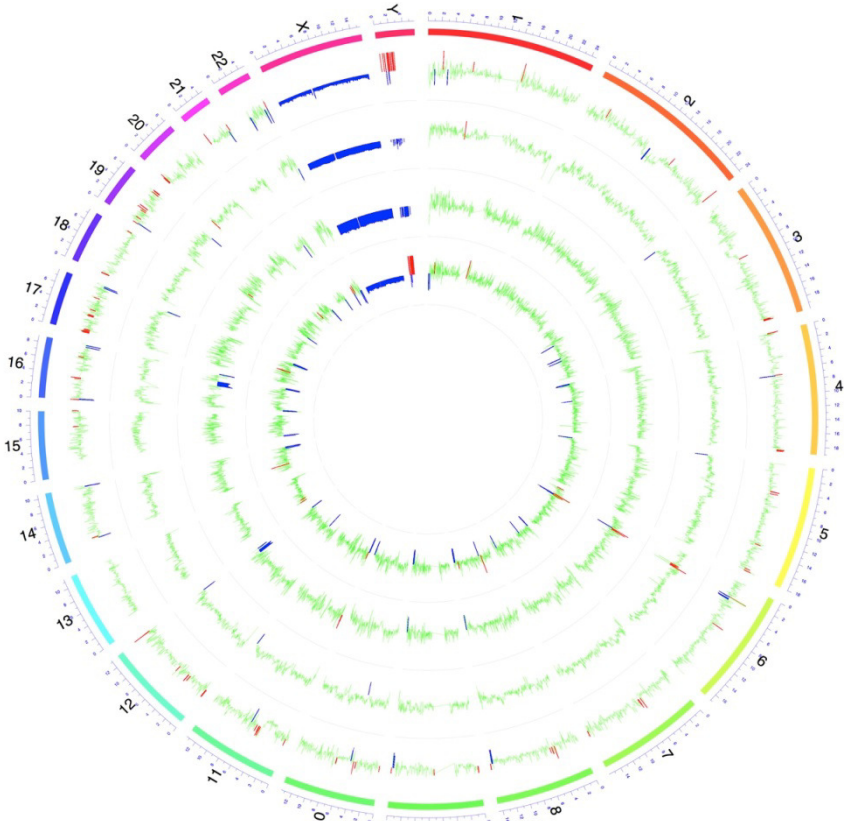

d

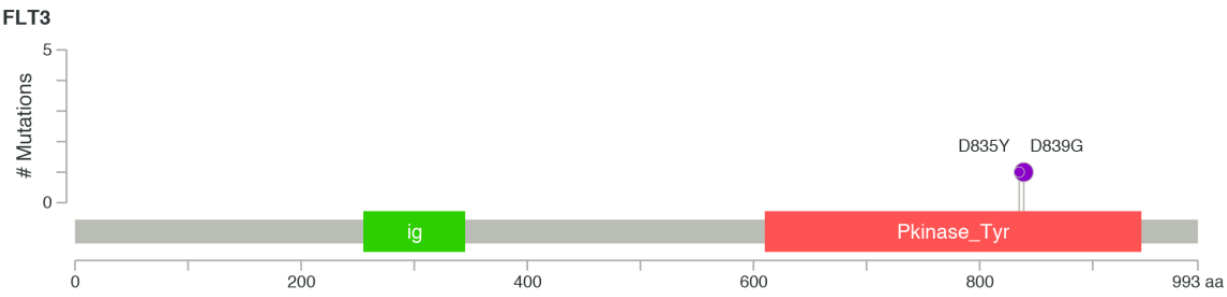

Suppl. Figure 11

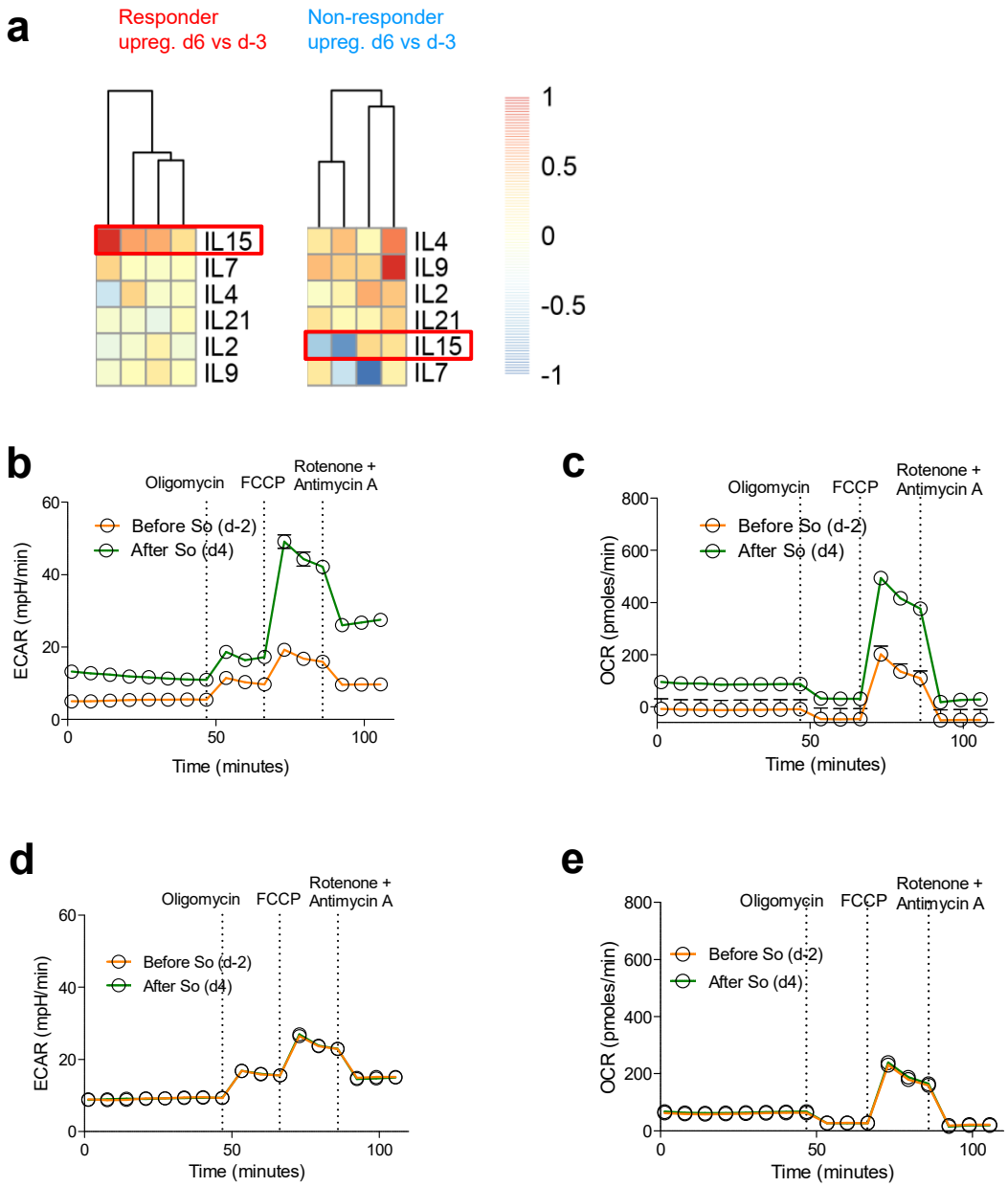

Suppl. Figure 12

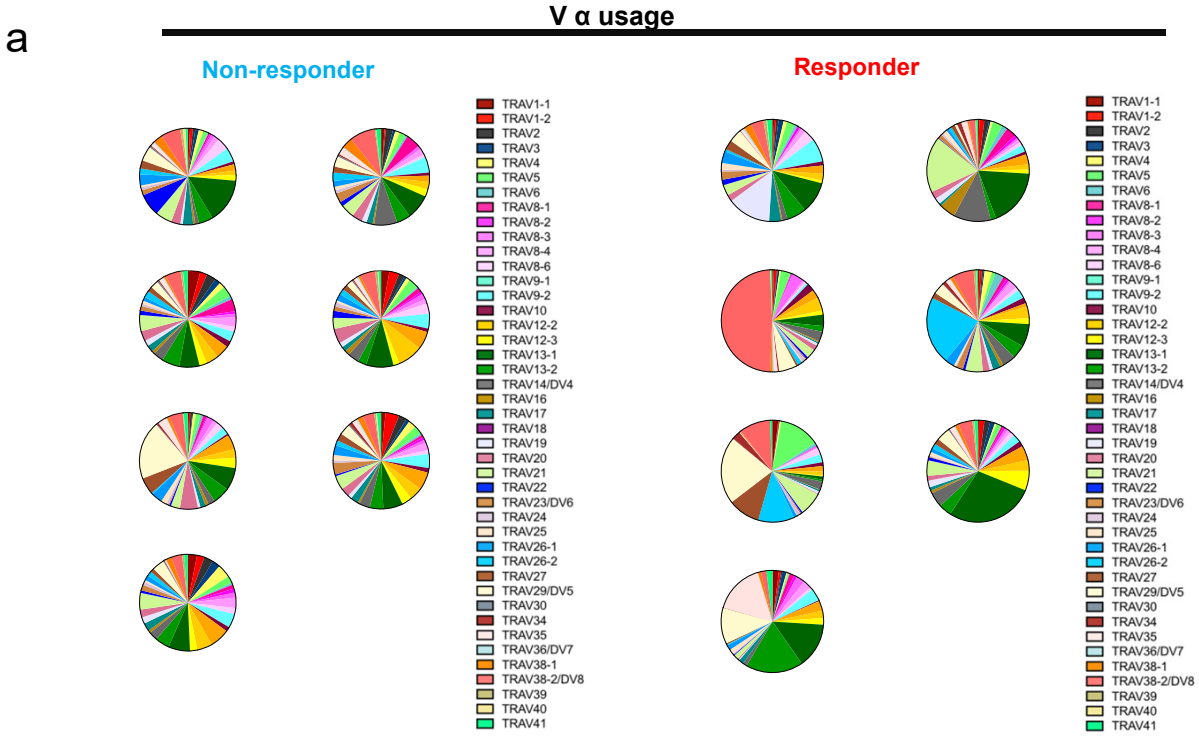

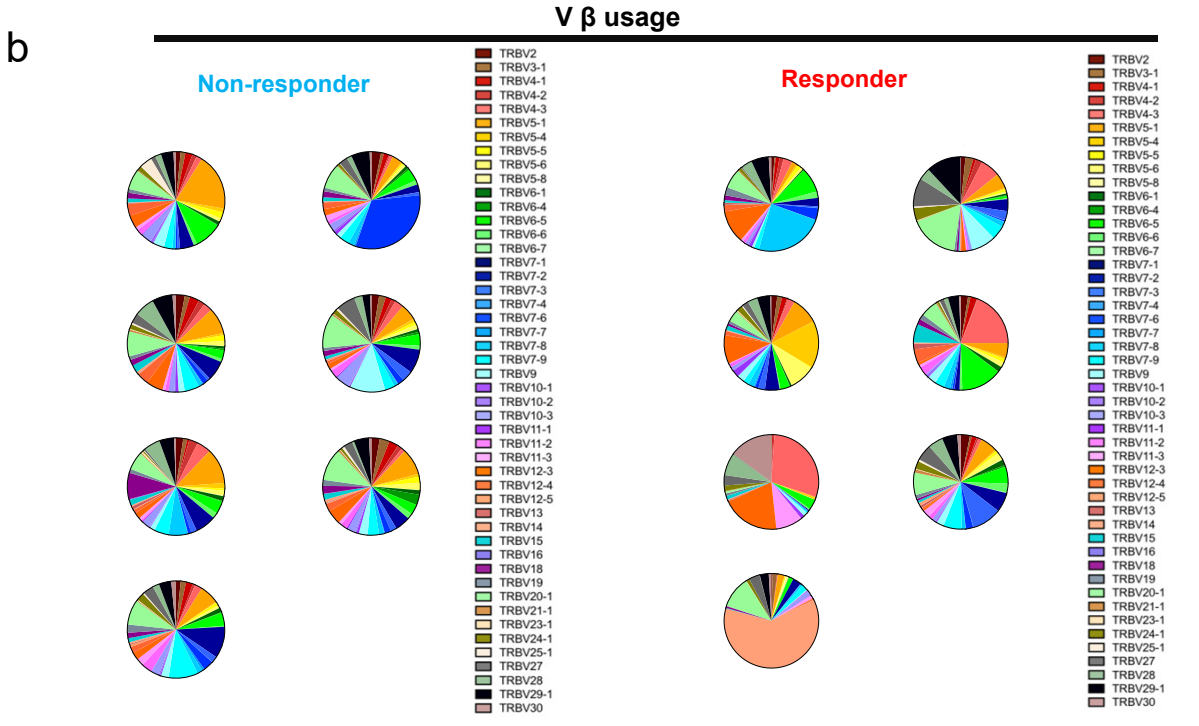

Suppl. Figure 13

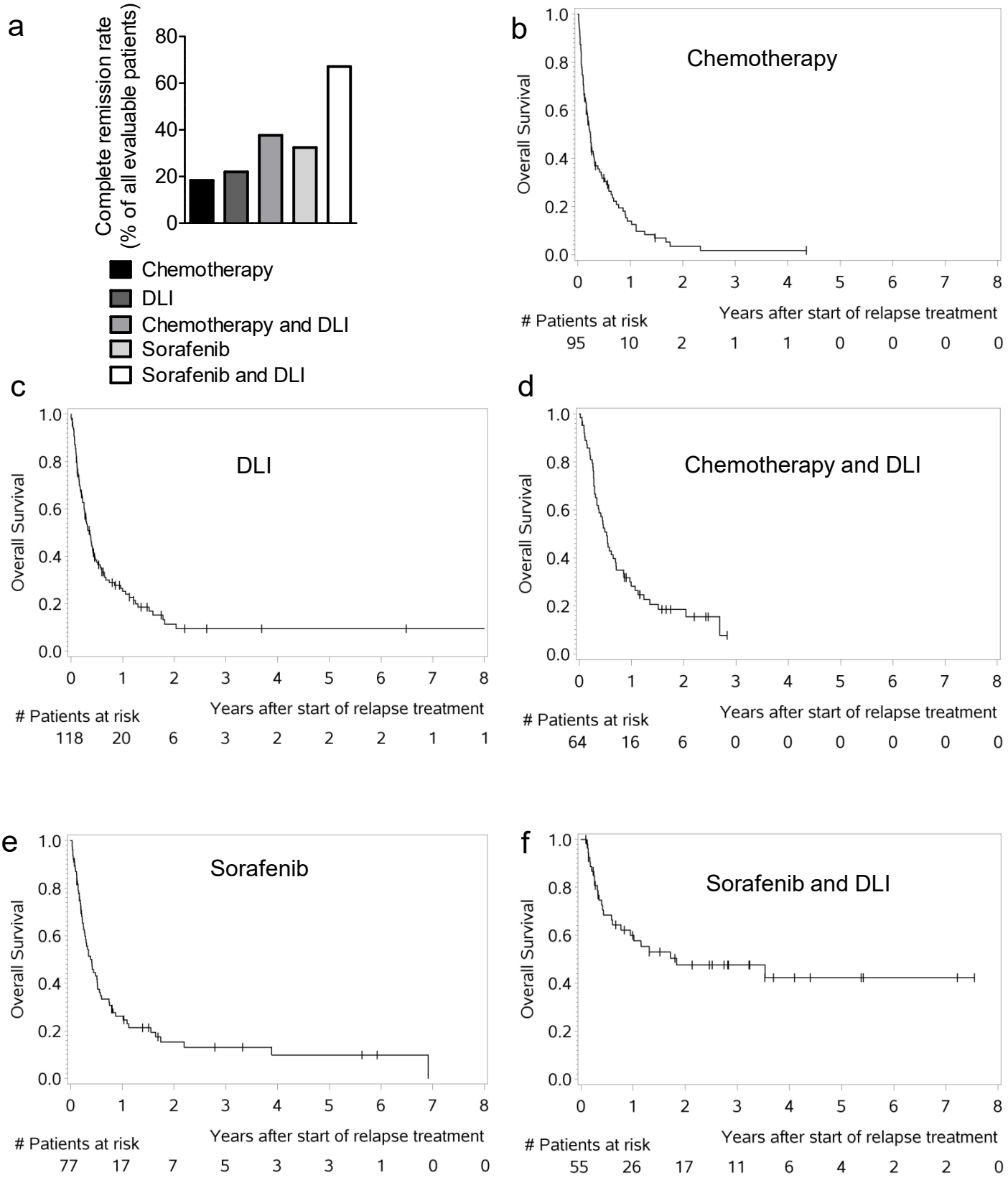

Suppl. Figure 14

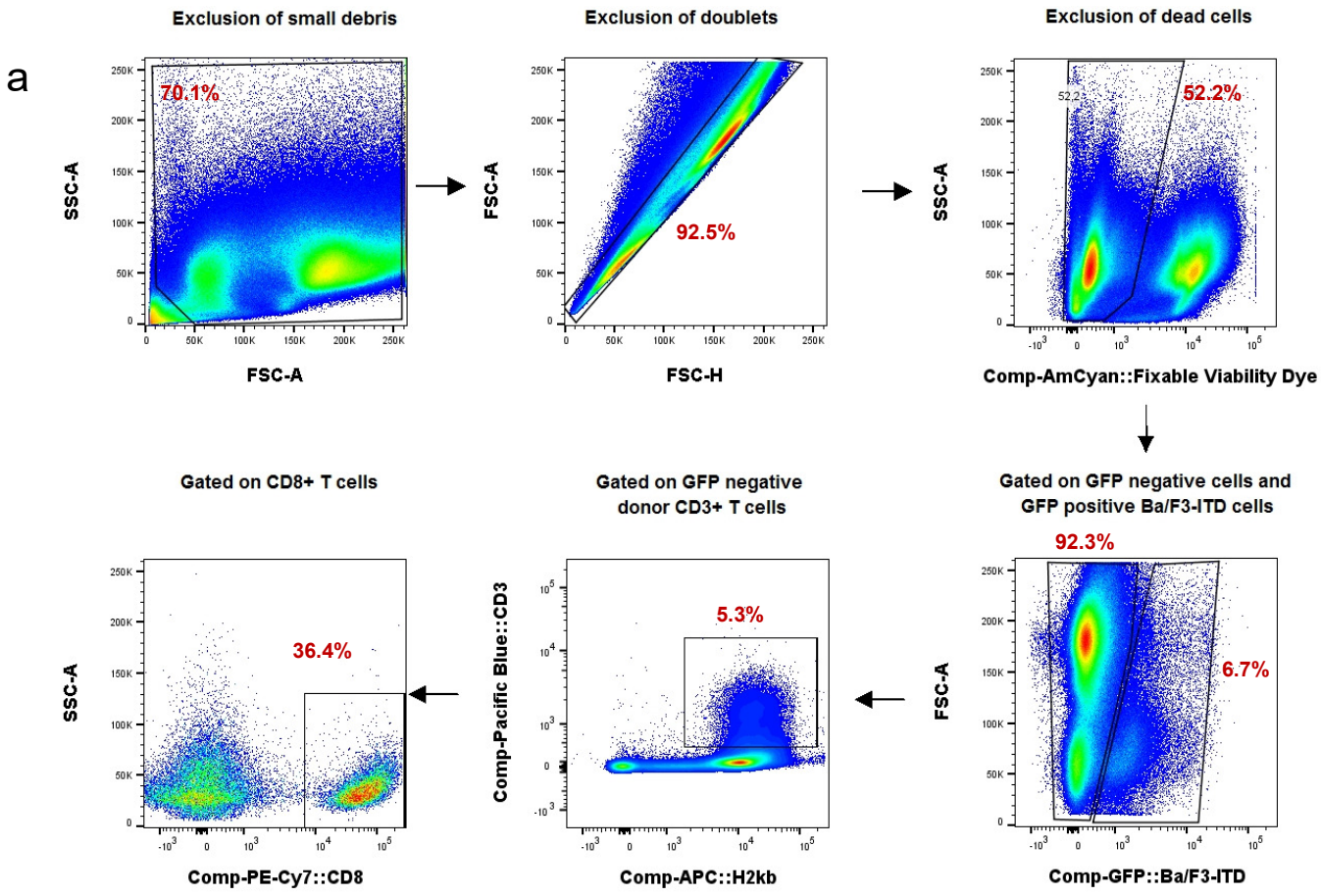

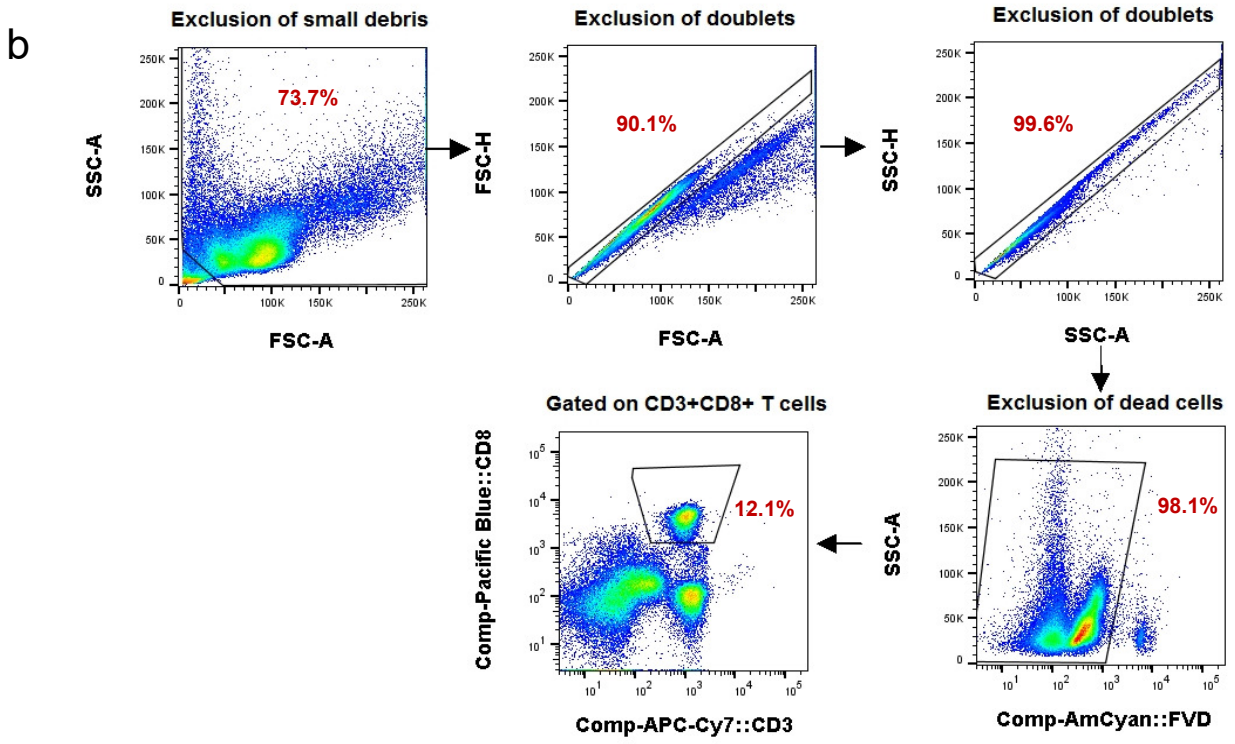

Suppl. Figure 15

WB shown in Figure 4c

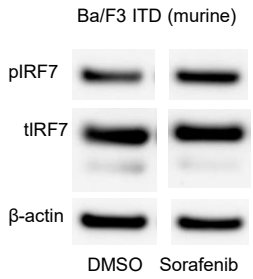

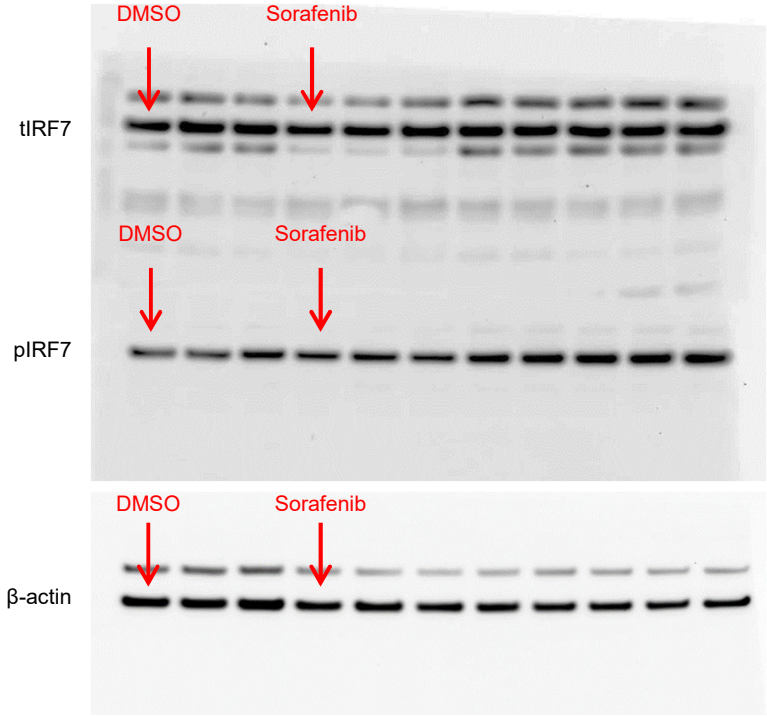

WB shown in Figure 4e

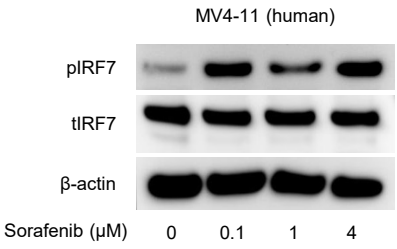

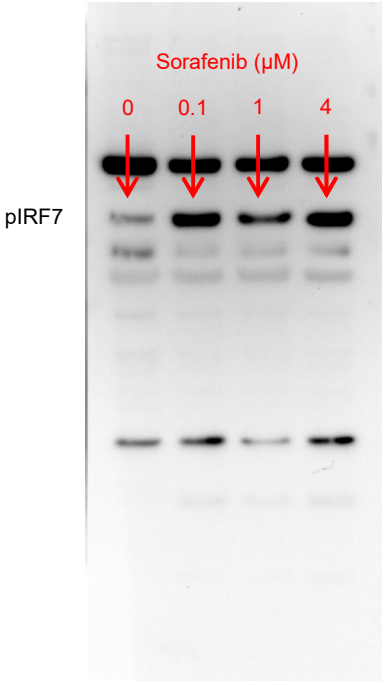

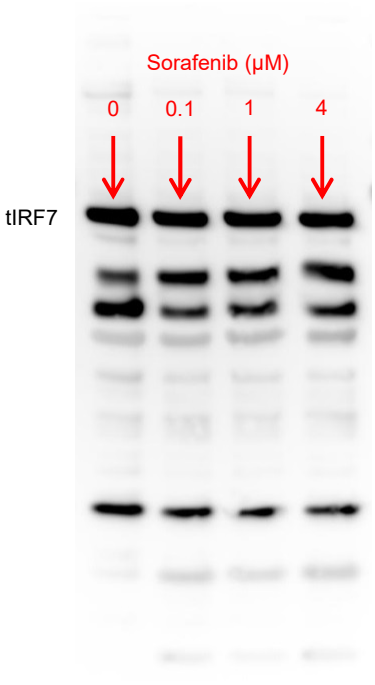

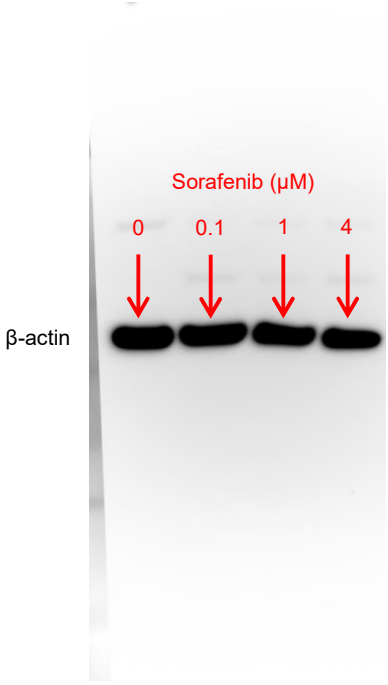

Suppl. Figure 16

WB shown in Suppl. Figure 4a

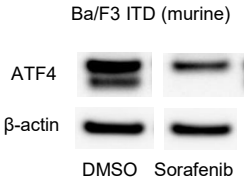

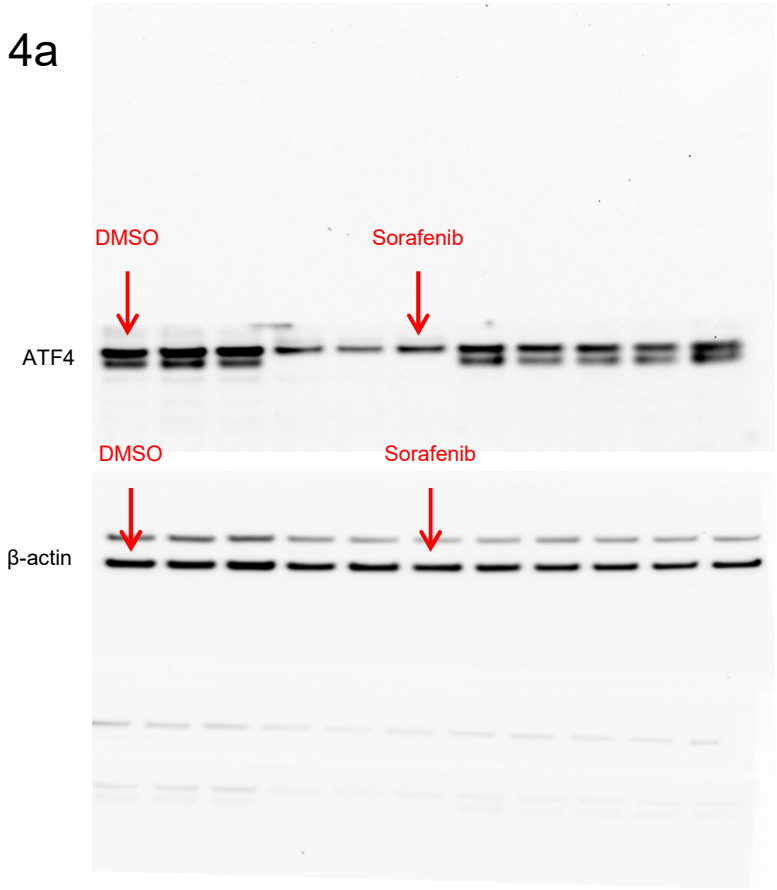

WB shown in Suppl. Figure 4b

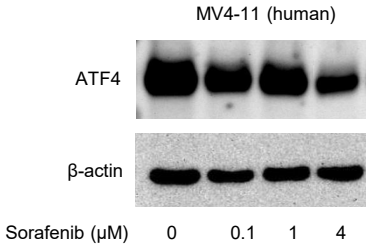

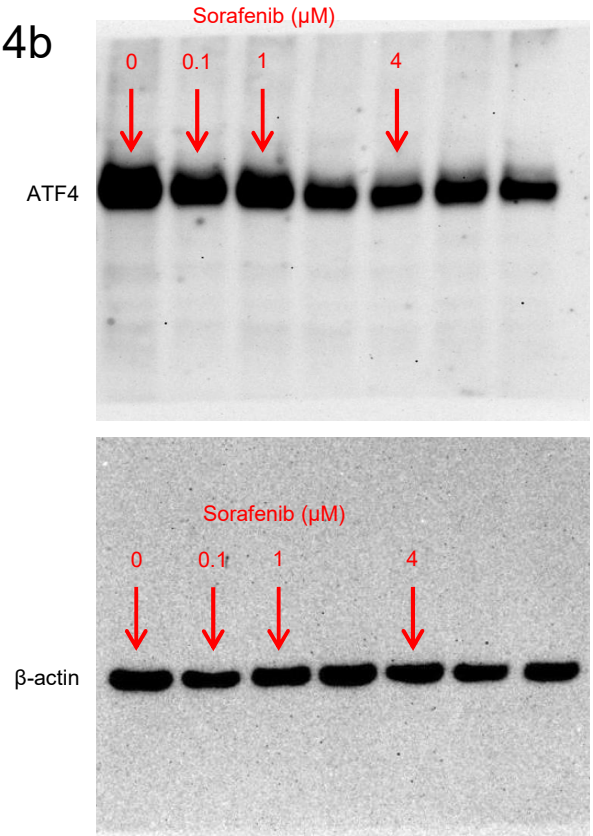

Suppl. Figure 17

WB shown in Suppl. Figure 4d

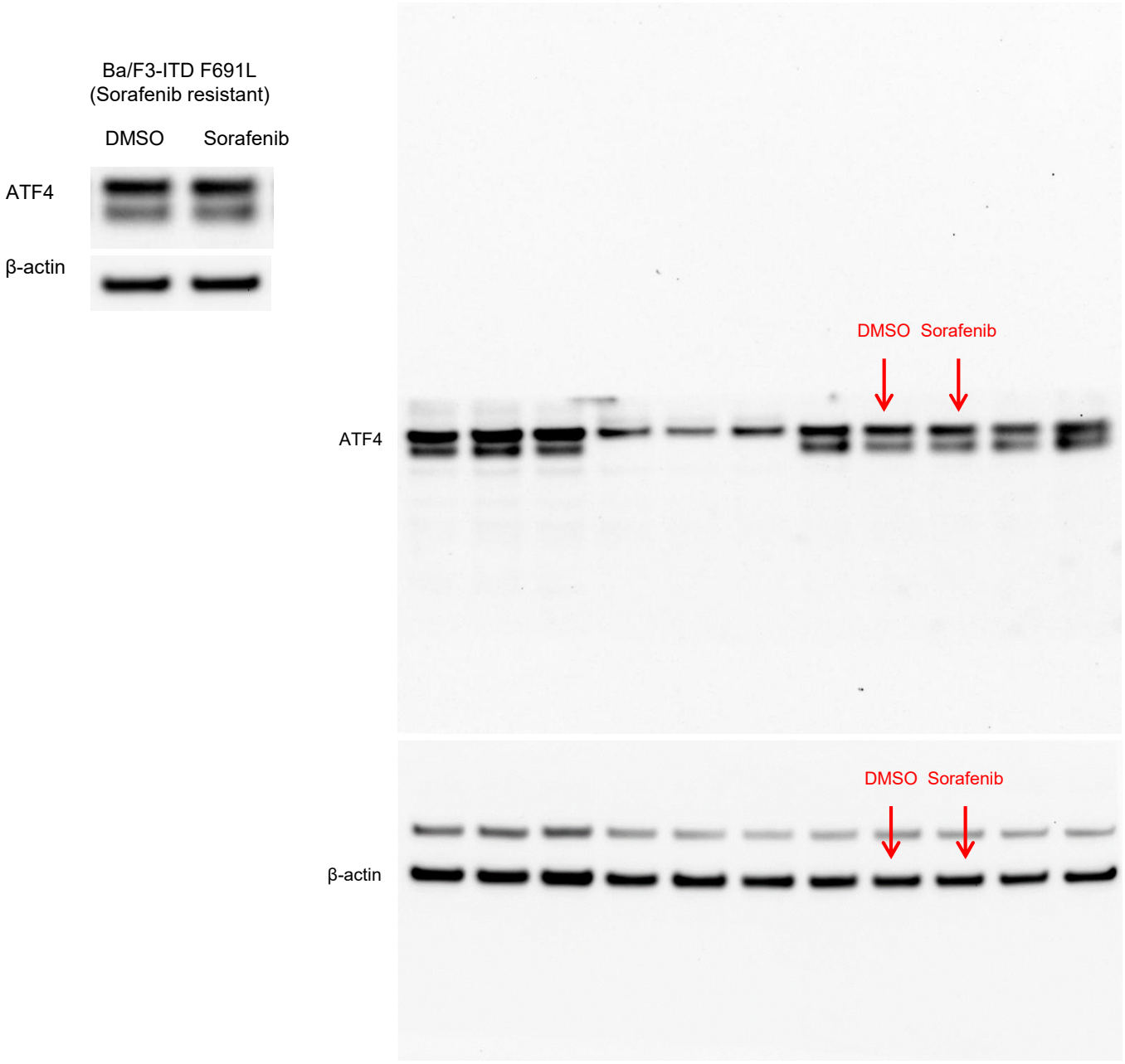

Suppl. Figure 18

WB shown in Suppl. Figure 4e

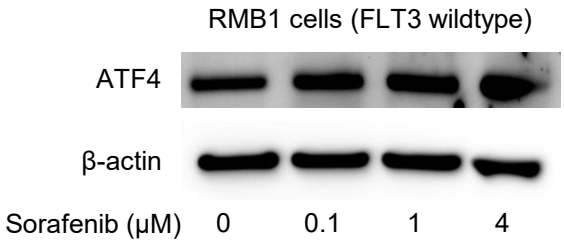

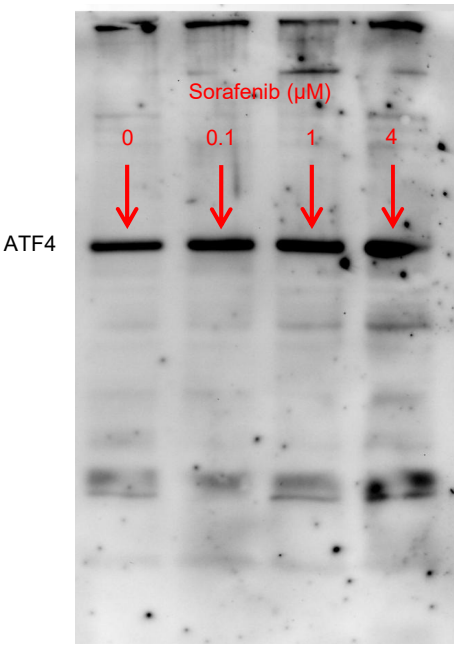

WB shown in Suppl. Figure 4f

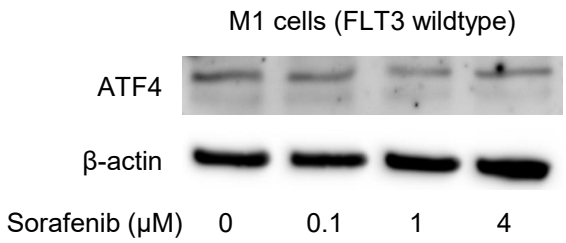

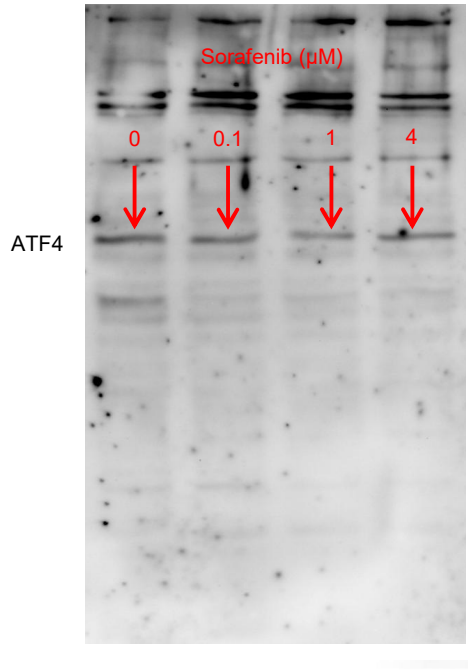

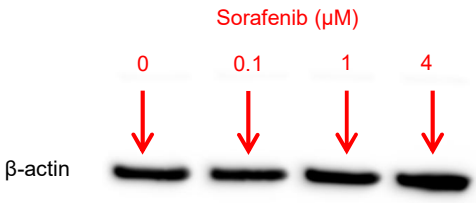

Suppl. Figure 19

WB shown in Suppl. Figure 4h

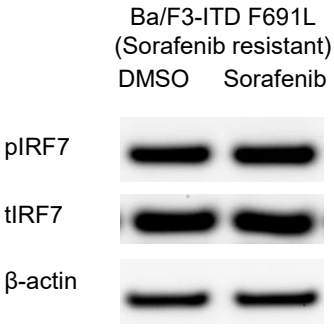

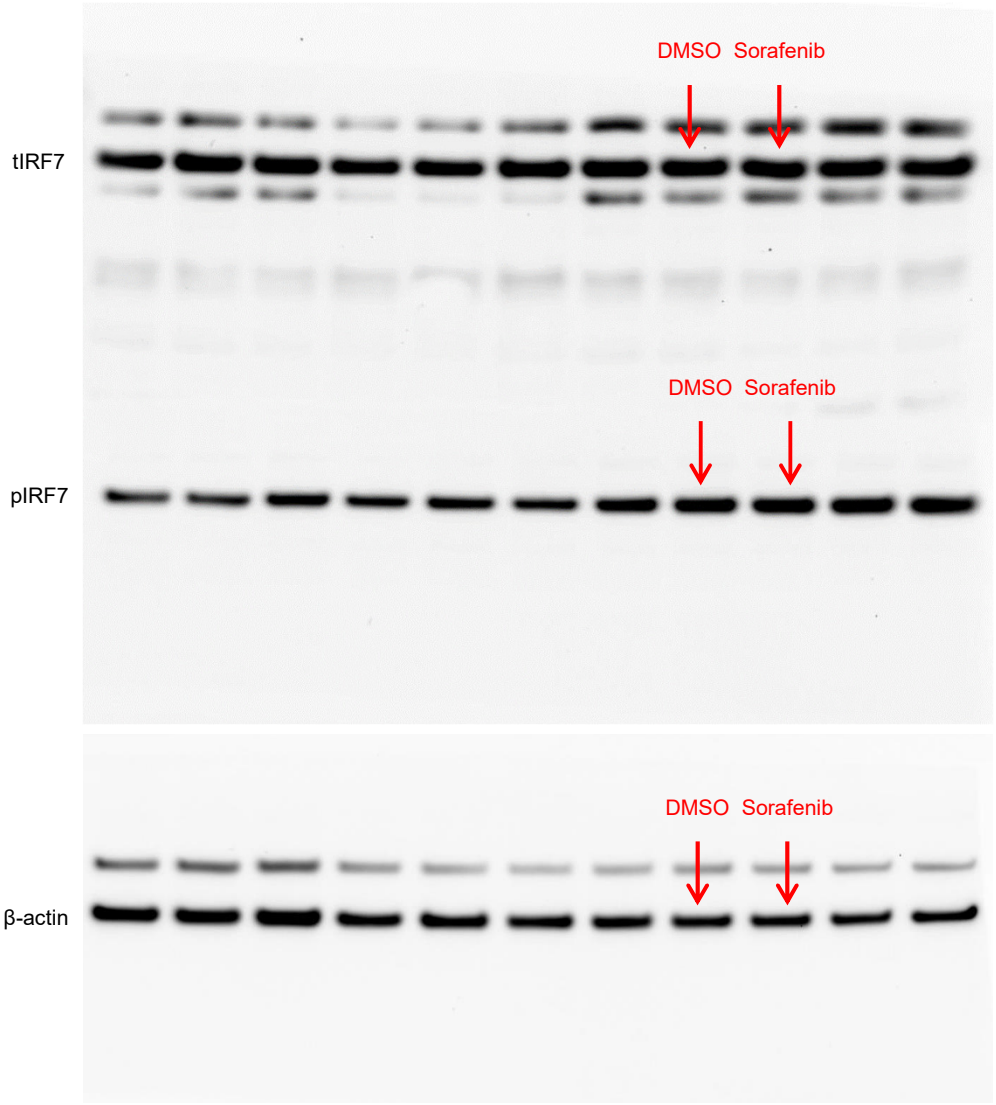

Suppl. Figure 20

WB shown in Suppl. Figure 4i

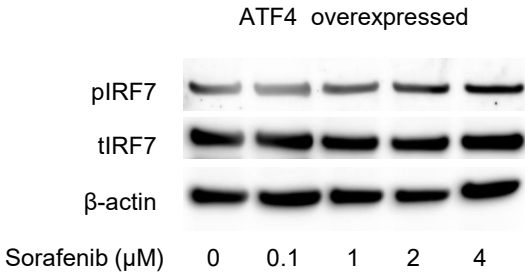

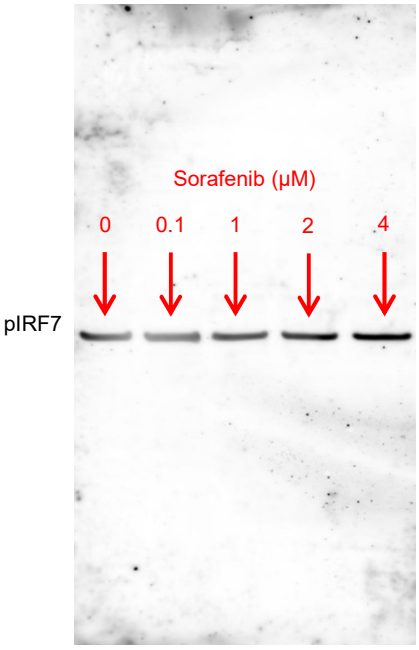

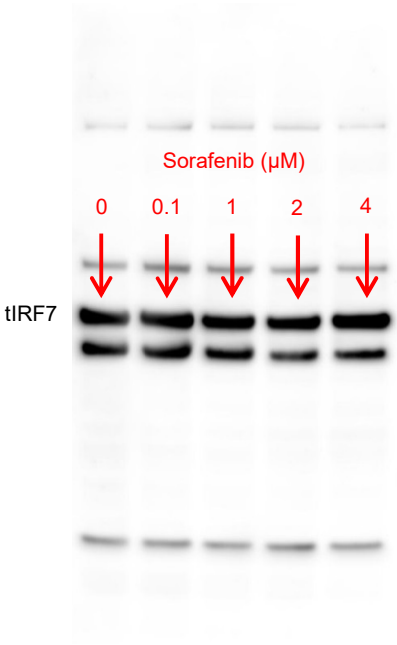

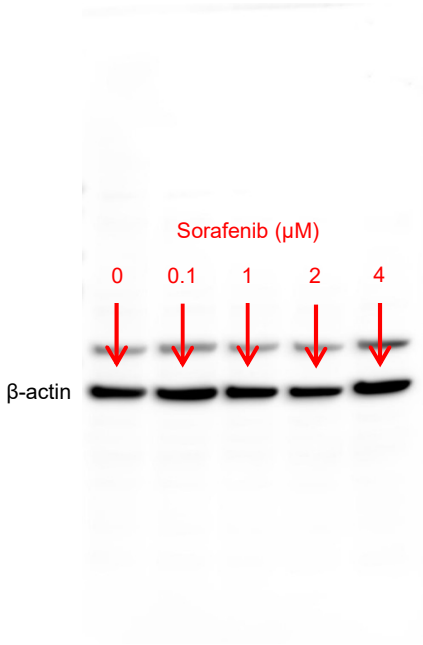

Suppl. Figure 21

WB shown in Suppl. Figure 4k

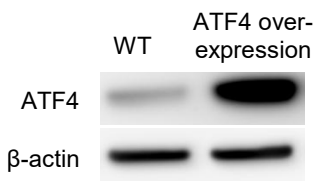

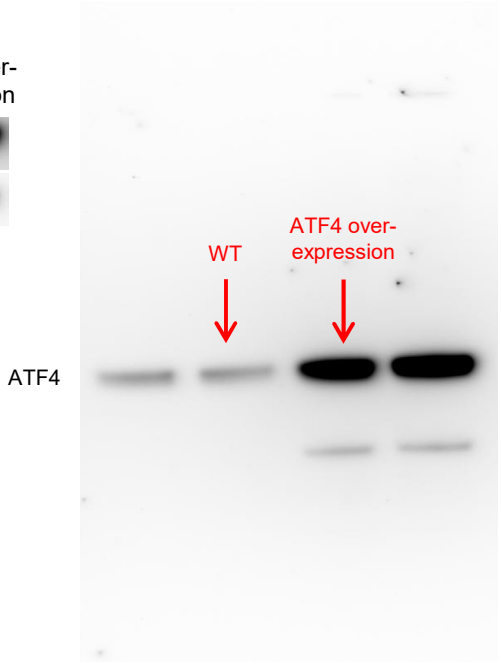

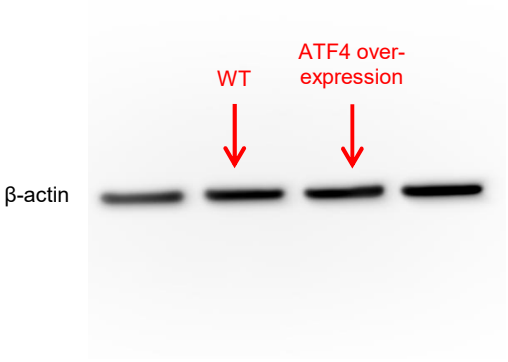

WB shown in Suppl. Figure 4l

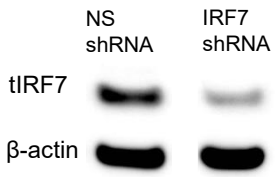

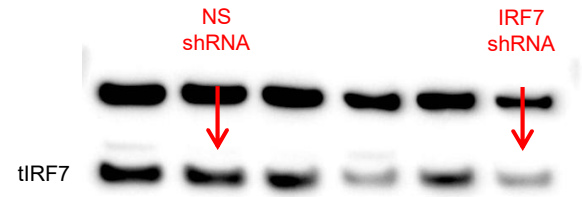

Supplementary Figure legends:

Suppl. Figure 1: Sorafenib induces IL-15 production in multiple FLT3-ITD mutant leukemia models

(a) Bioluminescence imaging (BLI) after Ba/F3-ITD^{luc} cell transplantation showing the expansion of Ba/F3-ITD^{luc} cells in BALB/c recipients transplanted with C57BL/6 BM and Tc and, treated with vehicle or sorafenib. Quantification of photons emitted per second from the Ba/F3-ITD^{luc} cells *in vivo* over time (mean ± s.e.m.). The experiment was repeated twice and the results were pooled; *n*=9 biologically independent animals per group at initial imaging (d3). The *P*-values are calculated using the two-sided Student's unpaired *t*-test.

(b) Quantification of IL-15/IL-15Rα (mean ± s.e.m.) in the serum from mice (C57BL/6) that were transplanted with GFP$^+$FLT3-ITD$^+$ transfected BM (C57BL/6) to induce leukemia, with additional BALB/c BM and Tc and treated with vehicle or sorafenib, on day 8 and day 14 following GFP$^+$FLT3-ITD$^+$ C57BL/6 BM injection. The experiment was performed once; *n*=6 biologically independent samples per group. The *P*-values were calculated by two-sided Student's unpaired t-test.

(c) Quantification of IL-15/IL-15Rα (mean ± s.e.m.) in the serum from BALB/c recipients transplanted with C57BL/6 BM / T-cells and WEHI-3B$^{FLT3\text{-}ITD}$ cells or WEHI-3B$^{empty\ vector}$-cells (BALB/c background). When indicated the mice were treated with vehicle or sorafenib. The number of mice analyzed per group are indicated after each group. The data (mean ± s.e.m.) are pooled from two independent experiments; BMT+Tc+Vehicle+WEHI-3B$^{empty\ vector}$ (n=13, biologically independent samples), BMT+Tc+Sorafenib+WEHI-3B$^{empty\ vector}$ (n=11, biologically independent samples), BMT+Tc+Vehicle+WEHI-3B$^{FLT3\text{-}ITD}$ (n=14, biologically independent samples), BMT+Tc+Vehicle+WEHI-3B$^{FLT3\text{-}ITD}$ (n=13, biologically independent samples). The *P*-values were calculated by two-sided Student's unpaired t-test.

(d) Quantification of IL-15/IL-15Rα (mean ± s.e.m.) in the serum from C57BL/6 recipients transplanted with BALB/c BM with or without AML$^{MLL\text{-}PTD\ FLT3\text{-}ITD}$ cells and additional BALB/c T-cells and treated with vehicle (*n*=12, biologically independent samples) or sorafenib (*n*=12, biologically independent samples) on day 14 following AML$^{MLL\text{-}PTD\ \ FLT3\text{-}ITD}$ cell and BM injection. The experiment was performed twice and the results (mean ± s.e.m.) were pooled. The *P*-values were calculated using the two-sided Mann-Whitney *U* test.

(e) Scatter plot showing the expression of CD107a (fold change of MFI with respect to mean MFI of DMSO treated controls) on all C57BL/6 mice-derived CD8$^+$ T-cells treated with DMSO or different concentrations of sorafenib for 24 hours as indicated in the figure. The experiment was performed twice and the results (mean ± s.e.m.) were pooled; *n*=6 biologically independent samples per group. The *P*-value was calculated using a two-sided Student's unpaired t-test; *P>0.05*, Not significant (*NS*).

(f) Scatter plot showing the expression of IFN-γ (fold change of MFI with respect to mean MFI of DMSO treated controls) on all C57BL/6 mice-derived CD8$^+$ T-cells treated with DMSO or different concentrations of sorafenib for 24 hours as indicated in the figure. The experiment was performed twice and the results (mean ± s.e.m.) were pooled; *n*=6 biologically independent samples per group. The *P*-value was calculated using a two-sided Student's unpaired t-test; *P>0.05*, Not significant (*NS*).

(g) A representative flow cytometry plot and the corresponding scatter plots representing the percentage of proliferated CD4$^+$ T-cells (left panel) and CD8$^+$ T-cells (right panel) on day 2

following their stimulation with CD3/CD28 beads and treatment with DMSO or different concentrations of sorafenib as indicated. The experiment was performed twice and the results (mean ± s.e.m.) were pooled; *n*=6 biologically independent samples per group. The *P*-value was calculated using a two-sided Student's unpaired t-test; *P>0.05*, Not significant (*NS*).

(h) Scatter plot showing the percentage of Annexin V and Fixable viability dye (FVD) double positive Ba/F3-ITD cells (target cells) co-cultured with C57BL/6 T-cells (effector cells) for 12 hours in different target to effector ratios as indicated. Only the T-cells were pretreated with different concentrations of sorafenib for 24 hours as indicated. Untreated Ba/F3-ITD cells were cultured without T-cells for 12 h and stained with Annexin V and FVD to detect background death of target cells. The experiment was performed twice and the results (mean ± s.e.m.) were pooled; *n*=6 biologically independent samples per group. The *P*-value was calculated using a two-sided Student's unpaired t-test; *P>0.05*, Not significant (*NS*).

(i) A representative flow cytometry plot showing the surface expression of IL-15Rα on $AML^{MLL\ PTD\ FLT3\ ITD}$ cells.

(j) Scatter plot showing the quantification of IL-15Rα on $AML^{MLL\ PTD\ FLT3\ ITD}$ cells (fold change of MFI with respect to mean MFI of isotype control). The experiment was performed twice and the results (mean ± s.e.m.) were pooled; *n*=6 biologically independent samples per group. The *P*-value was calculated using a two-sided Student's unpaired t-test.

Suppl. Figure 2: Sorafenib and IL-15 affect the T-cell phenotype.

(a, b) Flow cytometry analysis of the spleens of BALB/c mice transplanted with C57BL/6 BM, Ba/F3-ITD cells (day 0) and T-cells (C57BL/6, day 2) and treated with vehicle or sorafenib. The time point of analysis is day 12 following Ba/F3-ITD injection. **(a)** Representative flow cytometry plot showing the percentage of positive cells for the respective marker of all living donor ($H\text{-}2kb^+$) $CD8^+$ T-cells from BMT recipients treated with vehicle or sorafenib as indicated. **(b)** Scatter plots showing the quantification of positive cells for the respective marker of all living donor ($H\text{-}2kb^+$) $CD8^+$ T-cells from BMT recipients treated with vehicle or sorafenib as indicated. The experiment was performed three times and the results (mean ± s.e.m.) were pooled. The *P*-values were calculated using the two-sided Student's unpaired t-test; *P>0.05*, Not Significant (*NS*).

(c, d) CD107a levels in $CD8^+$ T-cells exposed for 24h to multiple concentrations of IL-15 or DMSO are shown. **(c)** Representative flow-cytometry plot showing the expression of CD107a in $CD8^+$ T-cells treated with DMSO or 200 ng/ml IL-15. **(d)** A representative scatter plot showing the expression of CD107a in $CD8^+$ T-cells which were treated with multiple concentrations of IL-15 as indicated in the graph. Pooled data from *n*=3 technical replicates is shown for one representative experiment. Similar results were obtained in two independent experiments.

(e) A representative flow cytometry plot showing the purity of the BM graft before and after depletion of $NK1.1^+$ cells. Similar results were obtained in two independent experiments.

(f) A representative flow cytometry plot showing the purity of splenic $CD3^+CD8^+H\text{-}2kb^+$ T-cells (92.2% of all living cells) of BALB/c mice which have received C57BL/6 BM and GFP^+ Ba/F3-ITD cells on day 0 and C57BL/6 Tc on day 2 is shown. Cells were isolated on day 12 following GFP^+ Ba/F3-ITD cell transfer. Similar results were obtained in four independent experiments.

(g) Survival rate of BALB/c mice ("secondary recipients") which received C57BL/6 BM ($5x10^6$ cells) and WEHI-$3B^{luc}$ cells (5000 cells) and were transplanted with or without additional H-$2kb^+CD3^+CD8^+$ T-cells from the spleens of BALB/c mice ("primary recipients") which received C57BL/6 BM and T-cells, and Ba/F3-ITD cells and treatment with either sorafenib or vehicle. The experiment was repeated twice and the results were pooled; *n*=10 biologically independent animals per group. *P*-values were calculated using the two-sided Mantel-Cox test; *P>0.05,* Not significant (*NS)*.
(h, i) Bioluminescence imaging (BLI) at different time points after WEHI-$3B^{luc}$ cell transplantation showing the expansion of WEHI-$3B^{luc}$ cells in different groups described in **(g)**. Representative images **(h)**, and quantification **(i)** of photons emitted per second from the WEHI-$3B^{luc}$ cells *in vivo* over time. The experiment was repeated twice and the results (mean ± s.e.m.) were pooled; *n*=10 biologically independent animals per group. The *P*-values were calculated using a two-sided Student's unpaired t-test for individual time points.

Suppl. Figure 3: Sorafenib does neither increase IL-15 production nor induce recall immunity in AML lacking FLT3-ITD mutations
(a) Scatter plots showing the quantification of IL-15 in the supernatant of different human-derived FLT3-$ITD^{negative}$ AML cell lines treated with different concentrations of sorafenib for 24 hours as indicated. The dotted line indicates the detection limit (2pg/ml) of the ELISA. *n*=3 technical replicates per group of one experiment are shown as representative data. The experiment was performed twice with similar results.
(b) Flow cytometry analysis for the intracellular expression of IL-15 in different mouse-derived FLT3-$ITD^{negative}$ AML cell lines treated with DMSO or sorafenib for 24 hours as indicated. Representative histograms for intracellular IL-15 expression and corresponding scatter plot indicating the quantification of intracellular IL-15 (fold change of MFI with respect to mean MFI of DMSO treated controls) in different FLT3-$ITD^{negative}$ AML cell lines (RMB1 and M1 cells) are shown. *n*=6 technical replicates per group are shown as representative data. The experiment was performed twice with similar results.
(c, d) BALB/c mice ("secondary recipients") which received C57BL/6 BM ($5X10^6$ cells) and WEHI-$3B^{luc}$ cells (100,000 cells) and transplanted with or without additional H-$2kb^+CD3^+$ $CD8^+$ T-cells from the spleens of BALB/c mice ("primary recipients") which received C57BL/6 BM and T-cells, and WEHI-$3B^{luc}$ cells and treated with either sorafenib or vehicle. **(c)** Shown are BLI images of representative mice from the different groups described above.
(d) Quantification of photons emitted per second from the WEHI-$3B^{luc}$ cells *in vivo* over time. The experiment was repeated twice with *n*=5 biologically independent animals per group and the results were pooled. The *P*-values were calculated for individual time points using a two-sided Student's unpaired *t*-test*,* Shown are mean and standard error of mean (s.e.m.), Not significant (*NS*).

Suppl. Figure 4: Sorafenib treatment does not increase the pIRF7/tIRF7 ratio when the leukemia cells have a sorafenib resistance mutation in FLT3 or have wildtype FLT3
(a) A representative Western blot showing the expression of ATF4 protein and loading control (β-actin) in murine Ba/F3-ITD (FLT3-ITD positive) cells treated with DMSO or sorafenib (0.1 µM) for 24h. Blot images were cropped and the two pieces are separated by a white border.

(b) A representative Western blot showing the expression of human ATF4 protein and loading control (β-actin) in human MV4-11 (FLT3-ITD positive) cells treated with the indicated sorafenib concentrations for 24 hours.
(c) Scatter plot showing the RMA values of *Atf4* in sorafenib-sensitive Ba/F3-ITD cells treated with DMSO or 10nM sorafenib for 24 hours. The *P*-values were calculated using a two-sided Student's unpaired t-test, *n*=6 biologically independent samples per group.
(d) Representative Western blots showing the expression of ATF4 in sorafenib-resistant Ba/F3-ITD cells (Ba/F3-ITD F691L) treated with DMSO or sorafenib (100 nM) for 24h. β-actin was used as a loading control. The experiment was performed twice with comparable results.
(e) Representative Western blot for ATF4 and loading control (β-actin) from the protein isolated from FLT3-wildtype murine RMB1 leukemia cells. The experiment was performed twice with comparable results.
(f) Representative Western blot for ATF4 and loading control (β-actin) from the protein isolated from FLT3-wildtype murine M1 leukemia cells. The experiment was performed twice with comparable results.
(g) Quantification of pIRF7/tIRF7 normalized to β-actin (fold change with respect to DMSO treated control) in MV4-11 cells (FLT3-ITD positive) treated with sorafenib as indicated. The experiment was repeated six times and the results (mean ± s.e.m.) were pooled; *n*=6 biologically independent samples per group (for the sorafenib concentrations 0.1 and 4 two values are close together and appear as "one" symbol due to overlay). The *P*-values were calculated using a two-sided Mann-Whitney U test.
(h) Representative Western blots showing the expression of pIRF7 and tIRF7 in sorafenib-resistant (F691L resistance mutation) Ba/F3-ITD cells treated with DMSO or sorafenib (100 nM) for 24h. β-actin was used as a loading control. The experiment was performed three times with comparable results.
(i) Representative western blot pIRF7, tIRF7 and loading control (β-actin) in Ba/F3-ITD cells transduced with a lentiviral vector overexpressing mouse ATF4 and treated with sorafenib at the indicated concentrations for 24 hours.
(j) Quantification of pIRF7/tIRF7 normalized to loading control (β-actin) (fold change with respect to DMSO treated control) in Ba/F3-ITD cells transduced with a lentiviral vector overexpressing mouse ATF4 and treated with sorafenib at the indicated concentrations for 24 hours. The experiment was repeated three times and the results (mean ± s.e.m.) were pooled; *n*=3 biologically independent samples per group. The *P*-values were calculated by the two-sided Mann-Whitney U test.
(k) Representative Western blot for ATF4 in the protein isolated from MV4-11 (human FLT3-ITD$^+$ AML cell line) cells containing an ATF4 overexpression vector or no vector as indicated. The experiment was performed four times with comparable results.
(l) Representative western blot for IRF7 in the protein isolated from MOLM-13 (human FLT3-ITD$^+$ AML cell line) cells that contained a non-silencing vector or an IRF7 knockdown vector. Blot images were cropped and the two pieces are separated by a white border. The experiment was performed two times with comparable results.
(m) Percentage of GFP$^+$ ATF4-overexpressing or ATF4-wildtype Ba/F3-ITD cells in the peripheral blood from different groups as indicated**.** The experiment was performed twice and the results (mean ± s.e.m.) were pooled; BM+Tc+Ba/F3-ITD$^{ATF4\text{-}Tg}$+Vehicle (*n*=10, biologically independent samples), BM+Tc+Ba/F3-ITD$^{ATF4\text{-}Tg}$+Sorafenib (*n*=9, biologically independent samples), BM+Tc+Ba/F3-ITD+Sorafenib (n=10, biologically independent samples). *P*-values were calculated using the two-sided Mann-Whitney U test.

Suppl. Figure 5: Analysis of the kinome in FLT3-ITD driven human leukemia cells
(a) Scatter plot diagram showing all kinases that detected by mass spectrometry in MV4-11 (FLT3-ITD positive) cells. The red kinases are those that are later chosen for functional studies. The data are derived from 3 technical replicates and the experiment was performed one time.

Suppl. Figure 6: Inhibition of kinases other than FLT3 does not induce IL-15 production
(a) Scatter plots showing normalized IL-15 levels (fold change of MFI with respect to mean MFI of DMSO controls) in Ba/F3-ITD cells (mouse, FLT3-ITD positive) treated with the indicated inhibitors. n=3 biologically independent samples (mean ± s.e.m.).
(b) Scatter plots showing IL-15 levels in the supernatant of human MV4-11 cells (human, FLT3-ITD positive) treated with the indicated inhibitors. n=3 biologically independent samples (mean ± s.e.m.). The dotted line indicates detection limit of human IL-15 ELISA (2pg/ml).

Suppl. Figure 7: Identification of kinases bound by sorafenib in human FLT3-ITD mutant leukemia cells
(a) Values for EC_{50}, K_d^{app} and R2 values for competitive Kinobead pulldown of sorafenib in MV4-11 lysate are shown.

Suppl. Figure 8: Different FLT3 inhibitors increase IL-15 production in FLT3-ITD$^+$ AML cells
(a) Scatter plot showing the quantification of intracellular IL-15 (fold change in MFI of IL-15 from inhibitor treated cells with respect to mean MFI of IL-15 from DMSO treated cells) in murine Ba/F3-ITD cells treated with different concentrations of tandutinib for 24h. n=12, biologically independent samples. The *P*-values were calculated using the two-sided Mann-Whitney U test.
(b) Scatter plot showing the quantification of *Il-15* mRNA by qPCR in the murine Ba/F3-ITD cells treated with different concentrations of tandutinib for 24h. n=9, biologically independent samples. The *P*-values were calculated using the two-sided Mann-Whitney U test.
(c) A representative western blot is shown for phospho FLT3 (pFLT3) in the murine Ba/F3-ITD cells treated with different concentrations of tandutinib for 24h. The experiment was independently performed twice with similar results.
(d) Scatter plot showing the quantification of intracellular IL-15 (fold change in MFI of IL-15 from inhibitor treated cells with respect to mean MFI of IL-15 from DMSO treated cells) in murine Ba/F3-ITD cells treated with different concentrations of midostaurin for 24h. n=9, biologically independent samples. The *P*-values were calculated using the two-sided Mann-Whitney U test.
(e) Scatter plot showing the quantification of *Il-15* mRNA by qPCR in the murine Ba/F3-ITD cells treated with different concentrations of midostaurin for 24h. n=6, biologically

independent samples. The *P*-values were calculated using the two-sided Mann-Whitney U test.
(f) A representative western blot is shown for phospho FLT3 (pFLT3) in the murine Ba/F3-ITD cells treated with different concentrations of midostaurin for 24h. The experiment was independently performed twice with similar results.
(g) Scatter plot showing the quantification of intracellular IL-15 (fold change in MFI of IL-15 from inhibitor treated cells with respect to mean MFI of IL-15 from DMSO treated cells) in murine Ba/F3-ITD cells treated with different concentrations of crenolanib for 24h. n=9, biologically independent samples. The *P*-values were calculated using the two-sided Mann-Whitney U test.
(h) Scatter plot showing the quantification of *Il-15* mRNA by qPCR in the murine Ba/F3-ITD cells treated with different concentrations of crenolanib for 24h. Crenolanib concentration 0 and 0.02 µM: n=8, biologically independent samples, crenolanib concentration 0.2 µM: n=7, biologically independent samples, crenolanib concentration 1 µM: n=6, biologically independent samples. The *P*-values were calculated using the two-sided Mann-Whitney U test.
(i) A representative western blot is shown for phospho FLT3 (pFLT3) in the murine Ba/F3-ITD cells treated with different concentrations of crenolanib for 24h. The experiment was independently performed twice with similar results.
(j) Scatter plot showing the quantification of intracellular IL-15 (fold change in MFI of IL-15 from inhibitor treated cells with respect to mean MFI of IL-15 from DMSO treated cells) in murine Ba/F3-ITD cells treated with different concentrations of quizartinib for 24h. n=9, biologically independent samples. The *P*-values were calculated using the two-sided Mann-Whitney U test.
(k) Scatter plot showing the quantification of *Il-15* mRNA by qPCR in the murine Ba/F3-ITD cells treated with different concentrations of quizartinib for 24h. quizartinib dosage 0 and 10: n=6, biologically independent samples, quizartinib concentration 1 nM and 100 nM: n=5, biologically independent samples. The *P*-values were calculated using the two-sided Mann-Whitney U test.
(l) A representative western blot is shown for phospho FLT3 (pFLT3) in the murine Ba/F3-ITD cells treated with different concentrations of quizartinib for 24h. The experiment was independently performed twice with similar results.
(m) Scatter plot showing the quantification of intracellular IL-15 (fold change in MFI of IL-15 from inhibitor treated cells with respect to mean MFI of IL-15 from DMSO treated cells) in murine Ba/F3-ITD cells treated with different concentrations of sorafenib for 24h. n=9, biologically independent samples. The *P*-values were calculated using the two-sided Mann-Whitney U test.
(n) Scatter plot showing the quantification of *IL-15* mRNA in human FLT3-ITD mutant myeloid MV4-11 cells exposed to quizartinib. The experiments were performed twice with similar results. n=6, biologically independent samples. The *P*-values were calculated using a two-sided Student's unpaired t-test.
(o) Scatter plot showing the quantification of *IL-15* mRNA in human FLT3-ITD mutant myeloid MV4-11 cells exposed to tandutinib. The experiments were performed twice with similar results. Concentration 0 µM: n=4, biologically independent samples. All other concentrations: n=6, biologically independent samples The *P*-values were calculated using a two-sided Mann-Whitney U test.
(p) The scatter plot represents the IL-15/IL-15Rα (mean ± s.e.m.) serum levels of BALB/c mice transplanted with C57BL/6 BM (d0) with additional injection of C57BL/6 T-cells (d2) on

day 12 following Ba/F3-ITD cells injection. As indicated for the respective scatter plots, mice were treated with either midostaurin (*n*=10, biologically independent samples), tandutinib (*n*=8, biologically independent samples), crenolanib (*n*=8, biologically independent samples), or vehicle (*n*=8, biologically independent samples). The experiment was independently performed twice and the results (mean ± s.e.m.) were pooled. The *P-values* were calculated by two-sided Student's unpaired t-test.
(q) Quantification of IL-15/IL-15Rα (mean ± s.e.m.) in the serum from BALB/c recipients transplanted with C57BL/6 BM / T-cells and WEHI-3B FLT3-ITD cells (BALB/c background). When indicated the mice were treated with vehicle or crenolanib. n=8, biologically independent samples. The data are pooled from 2 independent experiments. The *P*-values were calculated using the two-sided Mann-Whitney U test.

Suppl. Figure 9: Cytokine and chemokine levels under sorafenib treatment
(a, b) Representative images showing immunohistochemistry for pIRF-7 **(a)** and IL-15 **(b)** (positive cells in dark pink) from BM biopsies of FLT3-ITD$^+$ AML patients at diagnosis (upper panel), relapse after allo-HCT (middle panel), and after 10 days of sorafenib treatment (lower panel). The analysis was performed 3 times with similar results.
(c) Quantification of IL-15$^+$ cells/HPF in BM biopsies of FLT3-ITD$^+$ AML patients (responders *n*=12, biologically independent patients, non-responders, *n*=12, biologically independent patients) before (day 0) and during sorafenib-treatment (day 15 after start of treatment). Each data point indicates the measurement of an individual patient at the indicated time point. The *P*-value was determined by using the two-sided Wilcoxon matched-pairs signed rank test.
(d) IL-15 levels in the serum of patients relapsing with FLT3-ITD$^+$ AML after allo-HCT. Sorafenib/DLI responders (*n*=19, biologically independent patients) and non-responders (*n*=13, biologically independent patients) are shown separately. Data points indicate the IL-15 level in the serum of a patient on day 3 and day 30 after start of treatment. The dotted line in the graphs indicates the detection limit (4 pg/ml) of the IL-15 ELISA. The *P*-value was determined using the two-sided Wilcoxon matched-pairs signed rank test.
(e) TNF-α levels in the serum of patients relapsing with FLT3-ITD$^+$ AML after allo-HCT. Sorafenib/DLI responders (*n*=19, biologically independent patients) and non-responders (*n*=14, biologically independent patients) are shown separately Data points indicate the TNF-α level in the serum of a patient before (day 0) and during sorafenib treatment (day 3 after start of treatment). When using the two-sided Wilcoxon matched-pairs signed rank test no significant (*NS*) difference was found when pre- and post-sorafenib serum levels were compared.
(f) IL-12p70 levels in the serum of patients relapsing with FLT3-ITD$^+$ AML after allo-HCT. Sorafenib/DLI responders (*n*=19, biologically independent patients) and non-responders (*n*=14, biologically independent patients) are shown separately. Data points indicate the IL-12p70 level in the serum of a patient before (day 0) and during sorafenib treatment (day 3 after start of treatment). When using the Wilcoxon matched-pairs signed rank test no significant difference (*NS*) was found when pre- and post-sorafenib serum levels were compared.
(g) CXCL2 levels in the serum of patients relapsing with FLT3-ITD$^+$ AML after allo-HCT. Sorafenib/DLI responders (*n*=19, biologically independent patients) and non-responders (*n*=13, biologically independent patients) are shown separately. Data points indicate the CXCL2 level in the serum of a patient before (day 0) and during sorafenib treatment (day 3 after start of treatment). When using the two-sided Wilcoxon matched-pairs signed rank test

no significant (*NS*) difference was found when pre- and post-sorafenib serum levels were compared.
(h) CXCL5 levels in the serum of patients relapsing with FLT3-ITD$^+$ AML after allo-HCT. Sorafenib/DLI responders (*n*=19, biologically independent patients) and non-responders (*n*=14, biologically independent patients) are shown separately. Data points indicate the CXCL5 level in the serum of a patient before (day 0) and during sorafenib treatment (day 3 after start of treatment). When using the two-sided Wilcoxon matched-pairs signed rank test no significant (*NS*) difference was found when pre- and post-sorafenib serum levels were compared.
(i) CXCL6 levels in the serum of patients relapsing with FLT3-ITD$^+$ AML after allo-HCT. Sorafenib/DLI responders (*n*=19, biologically independent patients) and non-responders (*n*=13, biologically independent patients) are shown separately. Data points indicate the CXCL6 level in the serum of a patient before (day 0) and during sorafenib treatment (day 3 after start of treatment). When using the two-sided Wilcoxon matched-pairs signed rank test no significant difference (*NS*) was found when pre- and post-sorafenib serum levels were compared.
(j) Representative flow cytometry histograms for the median fluorescence intensity for IFN-γ in CD8$^+$ T-cells are shown for one sorafenib/DLI non-responder and one sorafenib/DLI responder. The experiment was performed one time.
(k) Quantification (MFI) of IFN-γ in CD8$^+$ T-cells derived from the peripheral blood of FLT3-ITD$^+$ AML patients (responders *n*=14, biologically independent patients, non-responders, *n*=12, biologically independent patients) before (day 0) and during sorafenib-treatment (day 3 after start of treatment) by flow cytometry. Each data point indicates the measurement of an individual patient at the indicated time point. Responders: IFN-γ (MFI) before versus after sorafenib, *P=0.01*. Non-responders: no significant difference before vs after sorafenib. The *P*-value was determined by using the two-sided Wilcoxon matched-pairs signed rank test.
(l) Representative flow cytometry histograms for the median fluorescence intensity for perforin in CD8$^+$ T-cells are shown for one sorafenib/DLI non-responder and one sorafenib/DLI responder. The experiment was performed one time.
(m) Quantification (MFI) of perforin in CD8$^+$ T-cells derived from the peripheral blood of FLT3-ITD$^+$ AML patients (responders *n*=14, biologically independent patients, non-responders *n*=12, biologically independent patients) before (day 0) and during sorafenib-treatment (day 3 after start of treatment) by flow cytometry. Each data point indicates the measurement of an individual patient at the indicated time point. Responders: perforin (MFI) before versus after sorafenib, *P=0.0006*. Non-responders: no significant difference before vs after sorafenib. The *P*-value was determined by using the two-sided Wilcoxon matched-pairs signed rank test.

Suppl. Figure 10: Whole genome sequencing of AML cells
(a-b) UpSet plots of the common and unique somatic mutations for two responder (Res, biologically independent patients) and two non-responder patients (NR, biologically independent patients). The number of somatic mutations is highly variable per patient, both for exonic (**a**) and intronic/exonic (**b**) mutations irrespective of the responder group, with few mutations being shared among patients.
(c) Circos plot of Copy Number Alterations (CNA) on Non Responders and responders AML samples. Each layer corresponds to one patient library. Bar height is proportional to copy

number, where green bars represent diploid condition, red and blue represent gain and loss, respectively.
(d) Schematic view of the FLT3 resistance mutations found in non-responders. Mutational allele frequency in two representative non-responders: P109S2E1: FLT3 D839G, VAF: 21.3% (23/109 reads), P108S2E1: FLT3 D835Y, VAF: 41.67% (45/108 reads)

Suppl. Figure 11: Gene expression analysis of AML cells and metabolism analysis of $CD8^+$ T-cells
(a) The heatmaps depict the scaled difference in the expression of common gamma chain interleukin genes. Six days (d6) after sorafenib treatment versus three days before (d-3) in AML cells. The left and right heatmaps show the difference for the responding (n=4, biologically independent patients) and non-responding patients (n=4, biologically independent patients), respectively. Genes were hierarchically clustered by their Euclidean distance using complete linkage algorithm.
(b) Time course for ECAR of $CD8^+$ T-cells (>90% purity) derived from the peripheral blood of a representative FLT3-ITD^+ AML patient who responded to sorafenib/DLI treatment before sorafenib treatment (day -2, orange line) and during sorafenib treatment (day 4 after start of treatment, green line). Data were combined from 5 technical replicates for this representative patient. The experiment was performed one time.
(c) Time course for OCR of $CD8^+$ T-cells (>90% purity) derived from the peripheral blood of a representative FLT3-ITD^+ AML patient who responded to sorafenib/DLI treatment before (day -2, orange line) and during sorafenib treatment (day 4 after start of treatment, green line). Data were combined from 5 technical replicates for this representative patient. The experiment was performed one time.
(d) Time course for ECAR of $CD8^+$ T-cells (>90% purity) derived from the peripheral blood of a representative FLT3-ITD^+ AML patient who did not respond (non-responder) to sorafenib/DLI treatment before sorafenib treatment (day -2, orange line) and during sorafenib treatment (day 4 after start of treatment, green line). Data were combined from 5 technical replicates for this representative patient. The experiment was performed one time.
(e) Time course for OCR of $CD8^+$ T-cells (>90% purity) derived from the peripheral blood of a representative FLT3-ITD^+ AML patient who did not respond (non-responder) before (day -2, orange line) and during sorafenib treatment (day 4 after start of treatment, green line). Data were combined from 5 technical replicates for this representative patient. The experiment was performed one time.

Suppl. Figure 12: TCR sequencing of isolated T-cells
(a, b) Usage of the variable α (TRAV, c) and β (TRBV, d) TCR genes for responders and non-responders is shown. Each pie chart represents an individual patient; different colors display different genes.

Suppl. Figure 13: Response rates and OS of patients treated for $AML^{FLT3\text{-}ITD}$ relapse after allo-HCT

(a) Complete remission rates of patients relapsing with FLT3-ITD mutant AML after allo-HCT, being divided into patients treated with Chemotherapy (95 patients, thereof in 3 cases response unknown, CR rate: 17 of 92 evaluable patients, 18.5%), DLI (118 patients, thereof in 18 cases response unknown, CR rate: 22 of 100 evaluable patients, 22%), Chemotherapy and DLI (64 patients, thereof in 1 case response unknown, CR rate: 23 of 63 evaluable patients, 36.5%), Sorafenib (77 patients, response known in all patients, CR rate: 25 of 77 patients, 32.5%), Sorafenib and DLI (55 patients, response known in all patients, CR rate: 37 of 55 patients, 67.3%).
(b-f) Overall survival (OS) of patients relapsing with FLT3-ITD mutant AML after allo-HCT, being divided in patients treated with different therapies as indicated.

Suppl. Figure 14: Gating strategy for identifying $CD8^+$ T-cells in human PBMC and murine spleen

a) Flow cytometry plot indicating the gating strategy to identify donor-derived ($H\text{-}2kb^+$) $CD3^+CD8^+$ T-cells from murine spleens. The gated cells were singlets, live (fixable viability dye negative) and GFP negative. The spleens are derived from mice which are transplanted with BM and Ba/F3-ITD cells (d0) and treated with allogeneic donor T-cells and vehicle or sorafenib (d2).

b) Flow cytometry plot indicating the gating strategy to identify $CD3^+CD8^+$ T-cells from human PBMC of FLT3-ITD AML patients. The gated cells were singlets and live (fixable viability dye (FVD) negative).

Suppl. Figure 15-21:

The uncut gels of all western blots displayed in Figure 4 and Suppl. Figure 4 are shown.

Suppl. Table 2: Treatment group that received only chemotherapy for relapse - Patients characteristics, molecular and cytogenetic characteristics of the AML

Total number of patients	95
Variable	
	median (range)
Pt. age in years	50 (14-76)
	% (absolute number)
Gender	
female	49.5 (47)
male	50.5 (48)
Cytogenetics	
Normal karyotype	70.5 (67)
Abnormal karyotype*	28.4 (27)
Unknown karyotype	1.1 (1)
Molecular genetics	
Normal (no mutation)	41.1 (39)
NPM1 mutant	36.8 (35)
NPM1 mutant and other mol. abnormality	4.2 (4)
Molecular abnormality other than NPM1*	6.3 (6)
Unknown	11.6 (11)
Remission status at transplant	
CR1	48.4 (46)
CR2	13.7 (13)
Refractory disease	15.8 (15)
Primary induction failure	7.3 (7)
Relapse	13.7 (13)
Not evaluable	1.1 (1)

* The karyotype and molecular abnormalities of each patient are provided in Suppl. Table 1 (excel table)

Abbreviations: Pt.: patients, CR1: First complete remission, CR2: second complete remission. Risk factors that we analyzed were chosen based on previously published literature: [1-5]

Suppl. Table 3: Treatment group that received only chemotherapy for relapse - Chemotherapy conditioning regimens and transplant characteristics

Variable	
Conditioning regimen	
MAC	20.0 (19)
RIC	80.0 (76)
Donor type	
MRD	41.1 (39)
MUD	29.4 (28)
MMUD	17.9 (17)
Haploidentical	4.2 (4)
Cord blood	7.4 (7)
Graft source	
PBSC	80.0 (76)
BM	12.6 (12)
Cord blood	7.4 (7)
Immunosuppression	
CNI	94.7 (90)
MMF	36.8 (35)
MTX	32.6 (31)
Campath	8.4 (8)
mTOR inhibitor	0
ATG	16.8 (16)
Post-Tx Cyclophos	6.3 (6)

Abbreviations: MAC: Myeloablative conditioning, RIC: reduced intensity conditioning, DLI: donor lymphocyte infusions, MRD: matched related donor, MUD: matched unrelated donor, MMUD: mismatched unrelated donor, PBSC: peripheral blood stem cells, BM: bone marrow, CNI: calcineurin inhibitor (tacrolimus, cyclosporine A), MMF mycophenolate mofetil, ATG: Anti Thymocyte globulin, MTX: methotrexate, n.s. means no significantly different value compared to the other group.
Post-Tx Cyclophos: post transplantation cyclophosphamide

Suppl. Table 4: Treatment group that received only DLI for relapse - Patients characteristics, molecular and cytogenetic characteristics of the AML

Total number of patients	118
Variable	
	median (range)
Pt. age in years	50 (12-76)
	% (absolute number)
Gender	
female	53.4 (63)
male	46.6 (55)
Cytogenetics	
Normal karyotype	70.4 (83)
Abnormal karyotype*	25.4 (30)
Unknown karyotype	4.2 (5)
Molecular genetics	
Normal (no mutation)	83.9 (99)
NPM1 mutant	14.4 (17)
NPM1 mutant and other mol. abnormality	0.85 (1)
Molecular abnormality other than NPM1*	0.85 (1)
Unknown	(0)
Remission status at transplant	
CR1	67.8 (80)
CR2	5.9 (7)
Refractory disease	10.2 (12)
Primary induction failure	1.7 (2)
Relapse	14.4 (17)
Not evaluable	(0)

* The karyotype and molecular abnormalities of each patient are provided in Suppl. Table 1 (excel table)

Abbreviations: Pt.: patients, CR1: First complete remission, CR2: second complete remission. Risk factors that we analyzed were chosen based on previously published literature: [1-5]

Suppl. Table 5: Treatment group that received only DLI for relapse - Chemotherapy conditioning regimens given before allo-HCT and transplant characteristics

Variable	
Conditioning regimen	
MAC	48.3 (57)
RIC	51.7 (61)
Donor type	
MRD	52.6 (62)
MUD	39.8 (47)
MMUD	1.7 (2)
Haploidentical	4.2 (5)
Cord blood	1.7 (2)
Graft source	
PBSC	79.7 (94)
BM	18.6 (22)
Cord blood	1.7 (2)
Immunosuppression	
CNI	94.1 (111)
MMF	34.7 (41)
MTX	44.9 (53)
Campath	0.85 (1)
mTOR inhibitor	5.1 (6)
ATG	44.1 (52)
Post-Tx Cyclophos	6.8 (8)

Abbreviations: MAC: Myeloablative conditioning, RIC: reduced intensity conditioning, DLI: donor lymphocyte infusions, MRD: matched related donor, MUD: matched unrelated donor, MMUD: mismatched unrelated donor, PBSC: peripheral blood stem cells, BM: bone marrow, CNI: calcineurin inhibitor (tacrolimus, cyclosporine A), MMF mycophenolate mofetil, ATG: Anti Thymocyte globulin, MTX: methotrexate, n.s. means no significantly different value compared to the other group.
Post-Tx Cyclophos: post transplantation cyclophosphamide

Suppl. Table 6: Treatment group that received chemotherapy and DLI for relapse - Patients characteristics, molecular and cytogenetic characteristics of the AML

Total number of patients	64
Variable	
	median (range)
Pt. age in years	52 (20-76)
	% (absolute number)
Gender	
female	51.6 (33)
male	48.4 (31)
Cytogenetics	
Normal karyotype	73.4 (47)
Abnormal karyotype*	26.6 (17)
Unknown karyotype	(0)
Molecular genetics	
Normal (no mutation)	53.1 (34)
NPM1 mutant	29.7 (19)
NPM1 mutant and other mol. abnormality	3.1 (2)
Molecular abnormality other than NPM1*	10.9 (7)
Unknown	3.1 (2)
Remission status at transplant	
CR1	65.6 (42)
CR2	9.4 (6)
Refractory disease	12.5 (8)
Primary induction failure	1.6 (1)
Relapse	10.9 (7)
Not evaluable	(0)

* The karyotype and molecular abnormalities of each patient are provided in Suppl. Table 1 (excel table)

Abbreviations: Pt.: patients, CR1: First complete remission, CR2: second complete remission. Risk factors that we analyzed were chosen based on previously published literature: [1-5]

Suppl. Table 7: Treatment group that received chemotherapy and DLI for relapse - Chemotherapy conditioning regimens and transplant characteristics

Variable	
Conditioning regimen	
MAC	28.1 (18)
RIC	71.9 (46)
Donor type	
MRD	54.7 (35)
MUD	37.5 (24)
MMUD	7.8 (5)
Haploidentical	(0)
Cord blood	(0)
Graft source	
PBSC	98.4 (63)
BM	1.6 (1)
Cord blood	(0)
Immunosuppression	
CNI	96.9 (62)
MMF	23.4 (15)
MTX	51.6 (33)
Campath	17.2 (11)
mTOR inhibitor	1.6 (1)
ATG	12.5 (8)
Post-Tx Cyclophos	(0)

Abbreviations: MAC: Myeloablative conditioning, RIC: reduced intensity conditioning, DLI: donor lymphocyte infusions, MRD: matched related donor, MUD: matched unrelated donor, MMUD: mismatched unrelated donor, PBSC: peripheral blood stem cells, BM: bone marrow, CNI: calcineurin inhibitor (tacrolimus, cyclosporine A), MMF mycophenolate mofetil, ATG: Anti Thymocyte globulin, MTX: methotrexate, n.s. means no significantly different value compared to the other group.
Post-Tx Cyclophos: post transplantation cyclophosphamide

Suppl. Table 8: Treatment group that received sorafenib (no DLI) for relapse - Patients characteristics, molecular and cytogenetic characteristics of the AML

Total number of patients	77
Variable	
	median (range)
Pt. age in years	53 (19-74)
	% (absolute number)
Gender	
female	53.2 (41)
male	46.8 (36)
Cytogenetics	
Normal karyotype	70.1 (54)
Abnormal karyotype*	28.6 (22)
Unknown karyotype	1.3 (1)
Molecular genetics	
Normal (no mutation)	39.0 (30)
NPM1 mutant	50.6 (39)
NPM1 mutant and other mol. abnormality	1.3 (1)
Molecular abnormality other than NPM1*	9.1 (7)
Unknown	(0)
Remission status at transplant	
CR1	36.3 (28)
CR2	10.4 (8)
Refractory disease	20.8 (16)
Primary induction failure	(0)
Relapse	32.5 (25)
Not evaluable	(0)

* The karyotype and molecular abnormalities of each patient are provided in Suppl. Table 1 (excel table)

Abbreviations: Pt.: patients, CR1: First complete remission, CR2: second complete remission. Risk factors that we analyzed were chosen based on previously published literature: [1-5]

Suppl. Table 9: Treatment group that received sorafenib (no DLI) for relapse - Chemotherapy conditioning regimens and transplant characteristics

Variable	
Conditioning regimen	
MAC	10.4 (8)
RIC	89.6 (69)
Donor type	
MRD	28.6 (22)
MUD	37.6 (29)
MMUD	16.9 (13)
Haploidentical	11.7 (9)
Cord blood	5.2 (4)
Graft source	
PBSC	88.3 (68)
BM	6.5 (5)
Cord blood	5.2 (4)
Immunosuppression	
CNI	85.7 (66)
MMF	41.6 (32)
MTX	39.0 (30)
Campath	5.2 (4)
mTOR inhibitor	11.7 (9)
ATG	35.1 (27)
Post-Tx Cyclophos	6.5 (5)

Abbreviations: MAC: Myeloablative conditioning, RIC: reduced intensity conditioning, DLI: donor lymphocyte infusions, MRD: matched related donor, MUD: matched unrelated donor, MMUD: mismatched unrelated donor, PBSC: peripheral blood stem cells, BM: bone marrow, CNI: calcineurin inhibitor (tacrolimus, cyclosporine A), MMF mycophenolate mofetil, ATG: Anti Thymocyte globulin, MTX: methotrexate, n.s. means no significantly different value compared to the other group.
Post-Tx Cyclophos: post transplantation cyclophosphamide

Suppl. Table 10: Treatment group that received sorafenib and DLI for relapse - Patients characteristics, molecular and cytogenetic characteristics of the AML

Total number of patients	55
Variable	
	median (range)
Pt. age in years	49 (18-68)
	% (absolute number)
Gender	
female	56.4 (31)
male	43.6 (24)
Cytogenetics	
Normal karyotype	87.3 (48)
Abnormal karyotype*	12.7 (7)
Unknown karyotype	(0)
Molecular genetics	
Normal (no mutation)	47.3 (26)
NPM1 mutant	49.1 (27)
NPM1 mutant and other mol. abnormality	(0)
Molecular abnormality other than NPM1*	1.8 (1)
Unknown	1.8 (1)
Remission status at transplant	
CR1	60.0 (33)
CR2	3.6 (2)
Refractory disease	21.8 (12)
Primary induction failure	(0)
Relapse	14.6 (8)
Not evaluable	(0)

* The karyotype and molecular abnormalities of each patient are provided in Suppl. Table 1 (excel table)

Abbreviations: Pt.: patients, CR1: First complete remission, CR2: second complete remission. Risk factors that we analyzed were chosen based on previously published literature: [1-5]

Suppl. Table 11: Treatment group that received sorafenib and DLI for relapse - Chemotherapy conditioning regimens and transplant characteristics

Variable	
Conditioning regimen	
MAC	29.1 (16)
RIC	70.9 (39)
Donor type	
MRD	25.5 (14)
MUD	47.2 (26)
MMUD	25.5 (14)
Haploidentical	1.8 (1)
Cord blood	(0)
Graft source	
PBSC	96.4 (53)
BM	3.6 (2)
Cord blood	(0)
Immunosuppression	
CNI	100 (55)
MMF	29.1 (16)
MTX	52.7 (29)
Campath	14.5 (8)
mTOR inhibitor	(0)
ATG	40.0 (22)
Post-Tx Cyclophos	3.6 (2)

Abbreviations: MAC: Myeloablative conditioning, RIC: reduced intensity conditioning, DLI: donor lymphocyte infusions, MRD: matched related donor, MUD: matched unrelated donor, MMUD: mismatched unrelated donor, PBSC: peripheral blood stem cells, BM: bone marrow, CNI: calcineurin inhibitor (tacrolimus, cyclosporine A), MMF mycophenolate mofetil, ATG: Anti Thymocyte globulin, MTX: methotrexate, n.s. means no significantly different value compared to the other group.
Post-Tx Cyclophos: post transplantation cyclophosphamide

Suppl. Table 12: Antibodies for flow cytometry

Antibody	Clone	Catalogue number	Flourochrome	Vendor	Citation
Anti-mouse CD3	17A2	100213	PB	Biolegend	[6]
Anti-mouse CD3	17A2	100233	BV510	Biolegend	[7]
Anti-mouse CD3ε	145-2C11	100309	PE-Cy5	Biolegend	[8]
Anti-mouse CD3	17A2	100215	Alexa flour 700	Biolegend	[9]
Anti-human CD3	SK7	344804	FITC	Biolegend	[10]
Anti-mouse CD4	RM4-5	100531	PB	Biolegend	[11]
Anti-mouse CD4	RM4-5	100549	BV711	Biolegend	[12]
Anti-mouse CD4	GK1.5	552051	APC-Cy7	BD Bioscience	[13]
Anti-mouse CD4	GK1.5	100408	PE	Biolegend	[14]
Anti-human CD45	H130	304022	PB	Biolegend	[15]
Anti-mouse CD8a	53-6.7	25-0081	PE-Cy7	eBioscience	[16]
Anti-mouse CD8a	53-6.7	560182	APC-H7	BD Bioscience	[17]
Anti-mouse CD8a	53-6.7	553030	FITC	BD Bioscience	[17]
Anti-mouse CD8a	53-6.7	100733	PerCP-Cy5.5	Biolegend	[18]
Anti-human CD8	BW135/80	130-094-152	VioBlue	Miltenyi	Supplier
Anti-mouse H-2kb	AF6-88.5.5.3	17-5958	APC	eBioscience	[19]
Anti-mouse H-2kb	AF6-88.5	116513	PB	Biolegend	[20]
Anti-mouse/human B220	RA3-6B2	103247	BV510	Biolegend	[21]
Anti-mouse Bcl-2	BCL/10C4	633511	PE-Cy7	Biolegend	[22]
Anti-mouse CD107a	1D4B	121612	PE	Biolegend	Supplier
Anti-mouse CD107a	1D4B	121613	APC	Biolegend	Supplier
Anti-human CD117	104D2	332785	PE	BD Bioscience	[23]
Anti-mouse Ly-6G/Ly-6C (Gr-1)	RB6-8C5	108412	APC	Biolegend	[24]
Anti-mouse IL-15Rα	DNT115Ra	12-7149	PE	eBioscience	[25]
Anti-mouse CD11b	M1/70	15-0112	PE-Cy5	eBioscience	[26]
Anti-mouse CD11b	M1/70	25-0112	PE-Cy7	eBioscience	[26]
Anti-mouse CD40L	MR1	106513	PerCP-Cy5.5	Biolegend	[27]
Anti-mouse F4/80	BM8	123112	PE-Cy5	Biolegend	[28]
Anti-mouse H2D(b)	KH95	553574	PE	BD Bioscience	[29]
Anti-mouse IFN-γ	XMG1.2	505825	PE-Cy7	Biolegend	[30]
Anti-mouse IFN-γ	XMG1.2	12-7311	PE	eBioscience	[31]
Anti-mouse IFN-γ	XMG1.2	17-7311	APC	eBioscience	[31]
Anti-human IFNγ	4S.B3	502512	APC	Biolegend	[32]
Anti-mouse IL-15	AIO.3	LS-C179458	Unconjugated	LifeSpan Biosciences	Supplier
Anti-mouse Ly-6C	AL-21	560525	PerCP-Cy5.5	BD Bioscience	[33]
Anti-mouse Ly-6C	HK1.4	128023	Alexa flour 700	Biolegend	[34]
Anti-mouse Ly-6G	1A8	127623	APC-Cy7	Biolegend	[35]
Anti-mouse NK1.1	PK136	108737	BV510	Biolegend	[36]

Anti-mouse NK1.1	PK136	108707	PE	Biolegend	[36]
Anti-mouse PD-1	RMP1-30	109109	PE-Cy7	Biolegend	[37]
Anti-mouse PD-1	29F.1A12	135219	BV605	Biolegend	[38]
Anti-human Perforin	B-D48	353316	PE-Cy7	Biolegend	[39]
Anti-STAT5 (pY694)	47/Stat5(pY694)	612567	PE	BD Bioscience	[40]

Abbreviations: PB: Pacific blue, BV: Brilliant violet, FITC: Fluorescein isothiocyanate, APC: Allophycocyanin, PE: Phycoerythrin, -Cy:-Cyanine, PerCP: Peridinin chlorophyll

Supplementary Methods

Additional information can be found at the "Life Sciences Reporting Summary"

Isolation of human Peripheral Blood Mononuclear Cells (PBMC)

Human blood was withdrawn into a sterile EDTA coated S-Monovette (Sarstedt, Germany). The blood was mixed with two volumes of 1X PBS and overlaid onto one volume of Pancoll Human (PAN-Biotech, Germany). A gradient centrifugation was performed at 440 xg for 30 minutes at room temperature to separate PBMC. The separated PBMC were collected and washed with 1X PBS for experimental use.

Isolation of $CD8^+$ T-cells from human PBMC

PBMC were isolated from human blood as described above. $CD8^+$ T-cells were enriched by positive selection with the MACS cell separation system (Miltenyi Biotec, USA) according to the manufacturer's instructions. Anti-human CD8 microBeads (Miltenyi Biotec, USA) were used. $CD8^+$ T-cell purity was at least 90% as assessed by flow cytometry.

TCR αβ Sequencing

PBMC were isolated from patients on day 30 after the start of sorafenib treatment. $CD3^+$ T-cells were enriched by positive selection with MACS separation system (Miltenyi Biotec, USA) according to manufacturer's instructions. Anti-human CD3 microbeads (Miltenyi Biotec, USA) were used. $CD3^+$ T-cell purity was at least 90% as assessed by flow cytometry. Total RNA was isolated from $CD3^+$ T-cells using RNeasy Mini kit or RNeasy Micro kit (QIAGEN, Netherlands) depending upon the number of cells obtained. RNA integrity was analyzed by capillary electrophoresis using a Fragment Analyser (Advanced Analytical Technologies, Inc. Ames, IA). Sequencing of the TCR α and β chains was performed on RNA by using a modified RACE PCR protocol[41,42]. cDNA was synthesized using the SmartScribe enzyme (Clontech) in the presence of biotinylated primers specific for the constant α and β chain genes and of a barcoded (5bp) template switching primer. TCR-specific cDNA molecules were captured with streptavidin magnetic beads (Dynabeads, Life Technologies), washed and resuspended in 10 µl water. 1 µl cDNA and 1 µl first PCR product were used as input material for the first and second exponential PCR, respectively. Fusion-primers harboring Illumina MiSeq sequencing adaptors were added in the second exponential PCR. Each individual sample was tagged with a barcoded (10 bp) fusion primer specific for the constant TCR genes. PCR amplicons were purified using the AmPure beads (Beckman Coulter) and sequenced with MiSeq paired-end 300 bp. After demultiplexing of the sequencing results, analysis of the TCR clonotypes was carried out using the MiTCR software[43]. Calculation of

the Shannon diversity index[44] was performed to determine the richness of a population represented by its total number of species (e.g. CDR3 aa sequences). Shannon index was calculated as follows: $SA = -\sum_i (n_i/N) \lg (n_i/N)$, where i is an index that is chosen between 1 and the number of species s, n_i is the number of sequencing reads in species i and N is the total number of reads.

Functional annotation of chromatin states

The functional annotation of the chromatin states was derived from a 15-state multivariate HMM that is based on five histone marks (H3K4me1, H3K4me3, H3K36me3, H3K27me3, H3K9me3) and 127 epigenomes from the epigenome roadmap consortium[45,46]. For characterization we used the data from primary monocytes from peripheral blood (Epigenome ID E029). All germline and somatic mutations within a given window around the respective gene transcription start sites were annotated according to one of the 15 states of the HMM model. Significance in mutation frequency differences between responder and non-responder groups was evaluated from an analysis of variance with posthoc Tukey's test.

Microarray analysis of murine leukemia cells

Ba/F3-ITD cells were treated with 10 nM sorafenib or DMSO for 24 hours. Total RNA was isolated using miRNeasy Mini kit (QIAGEN, Netherlands). Microarray analysis was performed as previously described[47]. The complete gene expression data are available at ArrayExpress accession number E-MTAB-4487.

ELISA for murine and human-derived cytokines and chemokines

The following ELISA kits were used according to manufacturer's protocol: Human IL-15 Quantikine ELISA Kit from R and D systems, and Human IL-15 ELISA ready-SET-Go! kit from eBioscience, Germany (human IL-15), Mouse IL-15/IL-15R Complex ELISA Ready-SET-Go! kit from eBioscience, Germany (murine IL-15), Human MIP2 ELISA Kit from Abcam, UK (human CXCL2), ELISA Kit for Granulocyte Chemotactic Protein 2 from Cloud-Clone Corp, China (human CXCL6), and Human IFN gamma ELISA Ready-SET-Go! kit from eBioscience, Germany (human IFN-γ). Human derived TNFα, IL-12p70 and CXCL5 were measured using custom-made LEGENDplex™ bead-based immunoassay (Biolegend, Germany) according to manufacturer's instruction.

***In vivo* administration of IL-15**

Recombinant murine IL-15 (210-15, Peprotech, Germany) was administrated i.p. at a dosage of 2.5 µg per mouse per day[48] from day 1 to day 7 following the injection of FLT3-ITD$^+$ BM cells.

In vivo depletion of IL-15

For systemic depletion of IL-15, anti-mouse IL-15/IL-15R complex functional grade purified antibody (Clone: GRW15PLZ; catalogue no: 16-8156-82, eBioscience, Germany)or isotype control antibody (LEAF™ purified rat IgG1κ isotype control antibody, Clone: RTK2071; catalogue no: 400414, Biolegend, Germany)[49] was administered i.p. at a dosage of 1 µg/g of body weight[49] on day 2, day 7 and day 15 following the transplantation of Ba/F3-ITD cells.

Recall immunity experiment

For the GvL recall immunity experiment, donor type $CD3^{+}CD8^{+}H\text{-}2kb^{+}$ T-cells were sorted by FACS from the spleens of BALB/c BMT recipients ($5x10^6$ BM cells, $2x10^5$ T-cells) on day 12 following the transplantation of Ba/F3-ITD cells (5000 cells) or WEHI-3B cells (100,000 cells). We injected $1x10^5$ sorted cells (purity of more than 90%) i.v. to secondary BALB/c recipients on day 2 following the transplantation of Ba/F3-ITD cells (5000 cells) or WEHI-3B cells (100,000 cells) and C57BL/6 BM ($5x10^6$).

Leukemic cell lines and cells

The following murine cell lines and cells were used: FLT3-ITD transfected Ba/F3 cells[50,51] (Ba/F3-ITD), FLT3-ITD and luciferase transfected Ba/F3-ITD cells ($Ba/F3\text{-}ITD^{luc}$), $AML^{MLL\ PTD\ FLT3\ ITD}$ leukemic cells[52], RMB1 (ACC 391)[53], M1 (ACC 331)[54] and luciferase and FLT3-ITD transfected WEHI-3B [55]. Ba/F3-ITD cells were provided by Dr. J. Duyster (Freiburg University Medical Centre) and $AML^{MLL\ PTD\ FLT3\ ITD}$ leukemic cells were provided by Dr. B. R. Blazar (University of Minnesota). The murine cell lines, RMB1 and M1 were purchased from DSMZ, Germany. The human cell lines, SKNO-1[56], KG-1[57], KG-1a[58], ML-2[59], HL-60[60], THP-1[61], KASUMI-1[62] and NB-4[63] were provided by Dr. M. Lübbert (Freiburg University Medical Centre) and MOLM-13 cells[64] were provided by Dr. T. Brummer (University of Freiburg). The human FLT3-ITD AML cell line MV4-11[64] was provided by Dr. J. Finke (Freiburg University Medical Centre). MV4-11 cells were shown to express exclusively the mutated FLT3 allele and constitutively phosphorylated receptor protein[64]. All the cell lines which were used for *in vivo* experiments were authenticated at DSMZ or Multiplexion, Germany. The human cell lines, MOLM-13 cells and MV4-11 cells were authenticated by STR profiling. The murine cell lines were authenticated by COI species analysis to trace them back to their donor mouse strains. All cell lines were tested repeatedly for Mycoplasma contamination and were found to be negative.

Graft Versus Leukemia Models

AML$^{\text{MLL-PTD FLT3-ITD}}$ leukemia model

For the AML$^{\text{MLL-PTD FLT3-ITD}}$ leukemia model[65], C57BL/6 recipients were transplanted with 5000 AML$^{\text{MLL-PTD FLT3-ITD}}$ cells and 5x10^6 BALB/c BM i.v. after lethal irradiation with 11 Gy in equally split doses. A total of 5x10^5 BALB/c (allogeneic model) or 2x10^5 BL/6 (syngeneic model) splenic CD4$^+$ and CD8$^+$ T-cells were introduced i.v. on day 2 following initial transplantation.

Ba/F3-ITD leukemia model

For the Ba/F3-ITD leukemia model, BALB/c recipients were transplanted with 5000 Ba/F3-ITD cells[51,66] and 5x10^6 C57BL/6 BM i.v. after lethal irradiation with 9 Gy in equally split doses. To induce GvL, a total of 2x10^5 C57BL/6 splenic WT or *Il-15Rα*$^{-/-}$ CD4$^+$ and CD8$^+$ T-cells were introduced i.v. on day 2 following initial transplantation.

For the Ba/F3-ITD$^{\text{ATF4-Tg}}$ (Ba/F3-ITD cells overexpressing ATF4) leukemia model, BALB/c recipients were transplanted with 500 Ba/F3-ITD $^{\text{ATF4-Tg}}$ cells and 5x10^6 C57BL/6 BM i.v. after lethal irradiation with 9 Gy in equally split doses. To induce GvL, a total of 2x10^5 C57BL/6 splenic CD4$^+$ and CD8$^+$ T-cells were introduced i.v. on day 2 following initial transplantation.

Transfection of primary mouse bone marrow with FLT3-ITD

To generate FLT3-ITD$^+$ BM cells C57BL/6 mice were injected with 150 mg kg^{-1} 5-fluorouracil (Medac GmbH) four days prior to bone marrow harvest. Whole bone marrow cells were infected with the MigR1 retroviral particles expressing FLT3-ITD and enhanced GFP[67] as previously described[68]. The GFP expressing cells were sorted and collected using a BD FACSAria III cell sorter (BD Bioscience, Germany).

WT C57BL/6 recipients were injected i.v. with 1.93x10^5 BALB/c BM and 7000 GFP$^+$ FLT3-ITD$^+$ C57BL/6 BM after lethal irradiation with 11 Gy in equally split doses. On day 2 after the initial transplantation 5x10^5 BALB/c splenic CD4$^+$ and CD8$^+$ T-cells were administered i.v.

When indicated *Il15*$^{-/-}$ recipients or *Il15*$^{-/-}$ BM (C57BL/6 background) were used instead of WT BM.

MV4-11 AML$^{\text{FLT3-ITD}}$ xenograft model

For the MV4-11 AML$^{\text{FLT3-ITD}}$ xenograft model[69], *Rag2*$^{-/-}$*Il2rγ*$^{-/-}$ recipients were transplanted with 25x10^4 MV4-11 cells i.v. after sublethal irradiation with 5 Gy in equally split doses. To induce GvL we injected a total of 2x10^5 C57BL/6 splenic CD4$^+$ and CD8$^+$ T-cells by i.v. on day 2 following the initial transplantation.

MOLM-13 AML$^{\text{FLT3-ITD}}$ xenograft model

For the MOLM-13 AML$^{\text{FLT3-ITD}}$ xenograft model[70], *Rag2*$^{-/-}$*Il2rγ*$^{-/-}$ recipients were transplanted with 25x10^3 MOLM-13$^{\text{NS shRNA}}$ i.v. after sublethal irradiation with 5 Gy in equally split doses.

When indicated $25x10^3$ MOLM-$13^{NS\ shRNA}$ or MOLM-$13^{IRF7\ shRNA}$ i.v. were used. The mice transplanted with MOLM-$13^{NS\ shRNA}$ or MOLM-$13^{IRF7\ shRNA}$ cells were given drinking water containing 2 mg/ml Doxycycline (Sigma-Aldrich, Germany) to induce the expression of NS shRNA or *Irf7* shRNA. To induce GvL we injected a total of $2x10^5$ C57BL/6 splenic $CD4^+$ and $CD8^+$ T-cells by i.v. on day 2 following the initial transplantation.

Primary AML$^{FLT3\text{-}ITD}$ xenograft model

AML reactive human $CD8^+$ T-cells were generated as previously described for $CD4^+$ T-cells[71]. Briefly, CD45RA-enriched $CD8^+$ T-cells (10^6/well) of an HLA-A2 negative healthy donor were stimulated weekly (d0, d7, d14 and d21) with irradiated HLA-A2 mismatch RNA-transfected autologous dendritic cells (DC) at a T-cell-to-DC ratio of 20:1 in 24-well plates in AIM-V medium (Life Technologies) supplemented with recombinant human interleukin (rhIL)-2 (50 IU/mL; Proleukin, San Diego, CA), rhIL-7 (5-10 ng/mL), and rhIL-15 (5 ng/mL); (both R&D Systems). In vitro-transcription of HLA-A*02:01 encoding RNA and electroporation of DC were performed as described[71]. On d21+4 of allo-HLA-A2/DC stimulation culture and prior to injection into mice, $CD8^+$ T-cells were analyzed for their reactivity to HLA-$A2^+$ primary AML blasts (AML151) in a standard [^{51}Cr]-release assay.

6 to 12-week-old female NSG mice were sublethally (1.5 Gy) y-irradiated one day prior to intravenous injection of $1x10^7$ primary AML151 blasts. On d21, a single dose of $1x10^6$ human T-cells (d21+4 of allo-HLA-A2/DC stimulation culture) was intravenously co-injected with rhIL-2 (1000 IU/mouse) and FcIL-7 (20 µg/mouse; Merck, Darmstadt, Germany). PBMC and leukemia blasts were isolated from buffy coat and leukapheresis products of healthy donors and AML patients at primary diagnosis and before the start of leukemia therapy after written informed consent, in accordance with the Declaration of Helsinki and after approval by the ethics committee of University Hospital Regensburg (permission number 13-101-0240 and 05-097, respectively).

***In vivo* bioluminescence imaging**

In vivo bioluminescence imaging was performed as described previously[72].

IL-15 measurement in the WEHI-3B AML model

The MigR1 retroviral particles expressing FLT3-ITD and enhanced GFP were prepared as described previously[67] and the target WEHI-3B cells were transduced as described previously[68]. The GFP expressing cells were sorted and collected using a BD FACSAria III cell sorter (BD Bioscience, Germany).

For the measurement of IL-15 in the WEHI-3B AML model, BALB/c recipients were transplanted with 100,000 WEHI-3B$^{empty\ vector}$ cells / WEHI-3B$^{FLT3\text{-}ITD}$ and 5x10^6 C57BL/6 BM i.v. after lethal irradiation with 9 Gy in equally divided doses. To induce GvL effects, we injected a total of 2x10^5 C57BL/6 splenic CD4$^+$ and CD8$^+$ T-cells by i.v. on day 2 following the initial transplantation.

Treatment with Kinase inhibitors

Sorafenib tablets were purchased from Bayer Pharma, Germany. Entospletinib (SYK inhibitor), ibrutinib (BTK inhibitor), vemurafenib (BRAF inhibitor), saracatinib (SRC inhibitor), KN-93 (CAMK2D inhibitor), Ro-3306 (CDK1 inhibitor), and FLT3 inhibitors (crenolanib, tandutinib, midostaurin and quizartinib) were purchased from Selleckchem, Germany.

For *in vitro* experiments, stocks of all inhibitors were dissolved in DMSO and used at appropriate dilutions as indicated in the figure legends. For *in vivo* experiments, pulverised sorafenib tablets and other inhibitors were dissolved in filter-sterilised vehicle solution consisting of 5% D-Glucose (AppliChem GmbH, Germany) and Poly(ethylene glycol) 300 (Sigma-Aldrich, Germany) in a 3:1 ratio, respectively. Sorafenib (daily dosage of 60 mg/kg of mouse body weight)[73], tandutinib (two times daily dosage of 20 mg/kg of mouse body weight)[74], midostaurin (daily dosage of 100 mg/kg of mouse body weight)[75] or vehicle was given to mice by oral gavage from day 2 until day12 or day 22 when indicated following transplantation of FLT3-ITD$^+$ leukemic cells. Crenolanib (daily dosage of 15 mg/kg of mouse body weight)[70] was given by intraperitoneal (i.p.) administration from day 2 until day 12 following transplantation of FLT3-ITD$^+$ leukemic cells.

Effect of Sorafenib on T-cell activation, cytotoxicity and proliferation *in vitro*

For T-cell activation and proliferation assay, CD4$^+$ and CD8$^+$ T-cells were isolated from the spleens of C57BL/6 mice using MACS. The T-cells were always plated in T-cell proliferation media (RPMI-1640+10% Fetal Calf serum +1% Pencillin-Streptomycin + 25 µM β-mercaptoethanol).

For T-cell activation, 200,000 T-cells were seeded in a 96 well plate and 4 µl of dynabeads mouse T-activator CD3/CD28 (Thermo Fischer Scientific, Germany) were added according to manufacturer's instruction. The T-cells were then incubated with different concentrations of sorafenib (0.1 µM and 1 µM) or DMSO for 24 hours. The cells were washed and stained for flow cytometry.

For T-cell proliferation assay, twice the amount of T-cells which has to be plated were stained with 5 µM celltrace violet dye in 1XPBS (celltrace violet cell proliferation kit , Thermo Fischer Scientific, Germany) for 20 minutes at room temperature in the dark. The reaction was stopped by diluting with five volumes of culture media and incubating for 5 minutes on

ice. The cells were pelleted by centrifugation and incubated for 10 minutes with pre-warmed fresh media before seeding. 200,000 of stained T-cells were seeded in a 96 well plate (day 0) and incubated with 4 µl of dynabeads mouse T-activator CD3/CD28 and different concentrations of sorafenib (0.1 µM and 1 µM) or DMSO. On day 2, the cells were analyzed for proliferation by flow cytometry.

To see the effect of sorafenib on T-cell cytotoxicity, T-cells (effector cells) were activated and pre-treated with different amounts of sorafenib (as described above) for 24 hours. The T-cells were washed and co-cultured with 200,000 Ba/F3-ITD cells (target cells) in different target to effector cell number ratios (200000:200000, 200000:400000, 200000:2000000) for 12 hours. The cells were washed and stained for Annexin V (Annexin V Apoptosis Detection Set PE-Cyanine7, eBioscience, Germany) and fixable viability dye eflour780 (eBioscience, Germany) according to manufacturer's instruction.

Western Blotting

Murine or human AML cell lines were treated with different inhibitors for 24 hours as mentioned in the figure legends and lysed using a radioimmunoprecipitation assay buffer (Santa Cruz Biotechnology, Heidelberg, Germany) supplemented with Phosphatase Inhibitor Cocktail 2 (Sigma-Aldrich, Germany). The protein concentration was determined using Pierce™ BCA Protein Assay Kit (Life Technologies, Germany). The protein samples were transferred onto nitrocellulose membranes (Amersham Biosciences, Germany) after running and resolving the total proteins in 4% to 12% sodium dodecyl sulphate-polyacrylamide electrophoresis gels (NuPAGE, Invitrogen, Germany). The membrane was incubated with blocking buffer (5% BSA in 1X tris buffer saline containing 0.1% tween-20) followed by incubation with primary antibodies diluted in blocking buffer. The primary antibodies used were anti-human/mouse phospho-FLT3 (Tyr589/591) (catalog no: 3464S, clone: 30D4)[76], anti-human ATF4 (catalog no: 11815S, clone: D4B8)[77], anti-human β-actin (catalog no: 4970, clone: 13E5)[78], anti-human phospho-IRF7 (Ser471/472) (catalog no: 5184, polyclonal)[79] from Cell Signaling Technology, USA and anti-mouse IRF7 (catalog no: ab109255, clone: EPR4718)[80] from Abcam, UK. Anti-rabbit IgG, HRP-linked Antibody (catalog no: 7074, Cell Signaling Technology, USA) was used as the secondary antibody. Lumigen ECL Plus (Lumigen, USA) was used as the chemoluminescent substrate. The signals from the blot are captured using the ChemoCam Imager 3.2 (Intas Science Imaging Instruments GmbH, Germany) and quantified using LabImage 1D software or ImageJ software.

Immunohistochemistry for IL-15 and phospho-IRF7 (pIRF7) from Human BM biopsies

Human BM smears were prepared on microscopic slides. For IL-15 staining, antigen retrieval was performed by cooking the slides in 1X Citrate buffer (pH=6) (Sigma-Aldrich, Germany) in a steamer for 20 minutes. For pIRF7 staining, antigen retrieval was performed by treating slides with 20 µg/ml Proteinase K solution for 8 minutes. After blocking with 10% goat serum for 30 minutes, slides were incubated specifically with primary antibodies, anti-IL15 (catalog no: ab55282, immunogen against recombinant full length protein corresponding to Human IL15 amino acid: 49-162, Abcam, USA)[81] and anti-pIRF7 (catalog no: bs3196R, polyclonal, Bioss Antibodies, USA)[82] for 30 minutes and 1 hour respectively. The slides were further incubated with corresponding secondary antibodies, polyclonal goat anti-rabbit immunoglobulins/biotinylated and polyclonal rabbit anti-mouse immunoglobulins/biotinylated (Dako, Germany) for pIRF7 and IL-15 respectively. The staining was detected using the Dako REAL™ Detection System, Alkaline Phosphatase/RED, Rabbit/Mouse (Dako, Germany). The slides were counterstained with hematoxylin (Merck,Germany) for 15 seconds and mounted using Roti ® -Histokitt mounting medium (Carl Roth, Germany).

Kinase enrichment using Kinet-1 Beads

MV4-11 cells were cultivated in RPMI supplemented with 10% FCS and 1% P/S and frozen as cell pellets ($100x10^6$ cells per pellet) at -80°C. Kinase enrichment was performed as described previously[83] with adaptations. Briefly, the cells were lysed on ice in lysis buffer (50 mM HEPES-NaOH pH7.5, 150 mM NaCl, 0.5% Triton-X 100, 1 mM EDTA, 1 mM EGTA) for 30 min supplemented with 10 mM NaF, 2.5 mM Na3VO4, PhosSTOPTM phosphatase inhibitor cocktail and cOmpleteTM protease inhibitor cocktail (Roche, Mannheim, Germany) and centrifuged at 16,000 xg for 30 min. Lysate protein concentration was measured using Bradford Assay Kit (Thermo Fisher Scientific, Germany) and adjusted to 2 mg/mL, and the NaCl concentration was adjusted to 1 M. As a control, 1 mL of lysate was incubated with 35 µL bead-bound pan-kinase inhibitor (Kinet-1) for 3h at 4°C on a rotating wheel. With each of the different washing buffers 3 washing steps were performed (Buffer 1: Lysis buffer stock + 1 M NaCl, 10 mM NaF, 0.1 mM Na3VO4; Buffer 2: Lysis buffer stock + 10 mM NaF, 0.1 mM Na3VO4; Buffer 3: 50 mM HEPES-NaOH (pH=7.5), 10 mM NaF, 0.1 mM Na3VO4) and the bead-bound kinases were eluted in 10 cycles. Each cycle consisted of incubating with 80 µL of a reducing elution buffer (ddH2O, 5 mM DTT, 0.5% SDS) at 60°C for 1 min, centrifugation and pooling eluates. Eluates were stored at -80°C until mass spectrometry analysis.

Mass spectrometry

Eluates were taken up in SDS lysis buffer and reduced with 1 mM DTT at 95°C, then alkylated with 5.5 mM iodoacetamide at room temperature in the dark, prior to separation by

SDS-PAGE using 4–12% Bis–Tris mini gradient gels (NuPAGE, Invitrogen, Darmstadt, Germany). The gel lanes were cut into 10 equal slices, the proteins therein were in–gel digested with trypsin (Promega, Mannheim, Germany), and the resulting peptide mixtures were processed on STAGE tips. Peptide samples were measured on a LTQ Orbitrap XL mass spectrometer (Thermo Fisher Scientific, Bremen, Germany) coupled to an Eksigent NanoLC-ultra. HPLC-column tips (fused silica) with a 75 µm inner diameter were self-packed with Reprosil-Pur 120 ODS-3 to a length of 20 cm. No pre-column was used. Peptides were injected at a flow of 500 nl/min in 92% buffer A (0.1% formic acid in water) and 2% buffer B (0.1% formic acid in acetonitrile). Separation was achieved by a linear gradient from 10% to 30% of buffer B at a flow rate of 250 nl/min. The mass spectrometer was operated in the data-dependent mode and switched automatically between MS (max. of 1 $x10^6$ ions) and MS/MS. Each MS scan was followed by a maximum of five MS/MS scans in the linear ion trap using a normalized collision energy of 35% and a target value of 5,000. Parent ions with a charge state of z = 1 and unassigned charge states were excluded from fragmentation. The mass range for MS was m/z = 370 to 2,000. The resolution was set to 60,000. MS parameters were as follows: spray voltage 2.3 kV; no sheath and auxiliary gas flow; ion transfer tube temperature 125^0C.

MS data analysis

The MS raw data files were uploaded into the MaxQuant software version 1.4.1.2 [84] which performs peak detection, generates peak lists of mass error corrected peptides, data base searches, and peptide and protein quantification. A full length Uniprot human database containing common contaminants, such as keratins and enzymes used for in-gel digestion, (based on Uniprot human version Jul. 2014) was employed, carbamidomethyl-cysteine was set as a fixed modification and methionine oxidation and protein amino-terminal acetylation were set as variable modifications. Three miss cleavages were allowed, enzyme specificity was trypsin/P, and the MS/MS tolerance was set to 0.5 Da. The average mass precision of identified peptides was in general less than 1 ppm after recalibration. Peptide lists were further used by MaxQuant to identify and relatively quantify proteins using the following parameters: peptide, and protein false discovery rates (FDR) were set to 0.01, maximum peptide posterior error probability (PEP) was set to 0.1, minimum peptide length was set to 7, minimum number of peptides for identification and quantitation of proteins was set to one, which must be unique, and identified proteins have been re-quantified. The “match-between-run” option (1 min) was used.

Binding profiling using affinity matrices

Methods were adapted from Klaeger et al. [85]. Kinobead selectivity profiling was performed as described previously [86]. Briefly, 5 mg of a protein of the MV4-11 cell line were incubated with sorafenib (S1040, Selleckchem) dilution series in DMSO (3 nM, 10 nM, 30 nM, 100 nM, 300 nM, 1 µM, 3 µM, 30 µM and DMSO) for 45 min at 4°C. The preincubation step was followed by incubation with kinobeads (35 µl settled beads). Bound proteins were eluted with LDS sample buffer (NuPAGE, Invitrogen) containing 50 mM DTT. For the calculation of a correction factor, the flowthrough of the DMSO control was incubated with fresh beads for a second time (pull down of pull down).

LC MS/MS analysis

Reduced eluates were alkylated with chloroacetamide (55 mM) and the proteins were concentrated by a short electrophoresis on a 4-12% NuPAGE gel (Invitrogen). In-gel digestion was performed according to standard procedures. Peptides generated by in-gel trypsin digestion were analyzed via LC-MS/MS on a nanoLC-Ultra 1D+ (Eksigent) coupled to a LTQ-Orbitrap Elite mass spectrometer (Thermo Scientific). Peptides were delivered to a trap column (100 µm x 2 cm, packed in house with Reprosil-Pur C18 AQ 5 µm resin, Dr. Maisch) at a flow rate of 5 µl/min in 100% solvent A0 (0.1% FA in HPLC grade water). Peptides were then separated on an analytical column (75 µm x 40 cm, packed in-house with Reprosil-Gold c18, 3 µm resin, Dr. Maisch) using a 100 min gradient ranging from 4-32% solvent B (0.1% FA and 5% DMSO in acetonitrile) in A1 (0.1% FA and 5% DMSO in HPLC grade water) at a flow rate of 300 nL/min. The mass spectrometer was operated in data dependent mode, automatically switching between MS and MS2 spectra. Up to 15 peptide precursors were subjected to fragmentation by higher energy collision-induced dissociation (HCD) and analyzed in the Orbitrap. An inclusion list for kinase peptides was enabled. Dynamic exclusion was set to 20 s.

Peptide and protein identification and quantification

Peptide and protein identification and quantification was performed using MaxQuant (version 1.5.3.30)[87] by searching the tandem MS data against a human Uniprot reference database (canonical entries, version 22.03.16, annotated in-house with PFAM domains) using the embedded search engine Andromeda[88]. Carbamidomethylated cysteine was used as fixed modification, phosphorylation of serine, threonine, and tyrosine, oxidation of methionine, and N-terminal protein acetylation as variable modifications. Trypsin/P was specified as the proteolytic enzyme and up to two missed cleavage sites were allowed. Precursor tolerance was set to 10 ppm and fragment ion tolerance to 0.05 Da. Label free quantification[89] and match between runs were enabled within MaxQuant. Search results were filtered for a

minimal length of seven amino acids, 1% peptide and protein FDR as well as common contaminants and reverse identifications.

Data analysis

For competition binding assays, EC50 values were determined based on the LFQ intensity ratio to the DMSO control for every single dose point and an in house generated R-Script [90,91], using nonlinear regression with variable slope. A K_d^{app} was then calculated by multiplying the EC_{50} with a correction factor for each protein. The correction factor (r) for a protein is defined as the ratio of the amount of protein captured from two consecutive of pull downs of the same DMSO control lysate.[86,92] Selected dose dependent inhibition curves were analyzed using GraphPad Prism (version 5.03).

References:

1. Bejanyan, N., Weisdorf, D.J., Logan, B.R., et al. Survival of AML patients relapsing after allogeneic hematopoietic cell transplantation: a CIBMTR study. *Biol Blood Marrow Transplant.* **21**, 454–459 (2015).
2. Barrett, J.A., Battiwalla, M. Relapse after allogeneic stem cell transplantation. *Expert Rev Hematol.* **4**, 429-441 (2010).
3. Boyiadzis, M., Arora, M., Klein, J.P.,et al. Impact of Chronic Graft-versus-Host Disease on Late Relapse and Survival on 7,489 Patients after Myeloablative Allogeneic Hematopoietic Cell Transplantation for Leukemia. *Clin Cancer Res.* **21**, 2020-2028 (2015).
4. Weisdorf, D., Zhang, M.J., Arora, M., Horowitz, M.M., Rizzo, J.D., Eapen, M. Graft-versus-host disease induced graft-versus-leukemia effect: greater impact on relapse and disease-free survival after reduced intensity conditioning. *Biol Blood Marrow Transplant.* **11**, 1727-1733 (2012).
5. Shimoni, A., Labopin, M., Savani, B., Volin L, Ehninger G, Kuball J, Bunjes D, Schaap N, Vigouroux S, Bacigalupo A, Veelken H, Sierra J, Eder M, Niederwieser D, Mohty M, Nagler A. Long-term survival and late events after allogeneic stem cell transplantation from HLA-matched siblings for acute myeloid leukemia with myeloablative compared to reduced-intensity conditioning: a report on behalf of the acute leukemia working party of European group for blood and marrow transplantation. *J Hematol Oncol.* **9**, 118 (2016).
6. Nagaoka, M., Hatta, Y., Kawaoka, Y., Malherbe, L.P. Antigen signal strength during priming determines effector CD4 T cell function and antigen sensitivity during influenza virus challenge. *J Immunol.* **193**, 2812-2820 (2014).
7. Cabrera-Perez, J., Condotta, S.A., James, B.R., et al. Alterations in antigen-specific naive CD4 T cell precursors after sepsis impairs their responsiveness to pathogen challenge. *J Immunol.* **194**, 1609-1620 (2015).

8. Qi, Q., Xia, M., Hu, J., Hicks E, Iyer A, Xiong N, August A. Enhanced development of CD4+ gammadelta T cells in the absence of Itk results in elevated IgE production. *Blood* **114**, 564-571 (2009).
9. Everard, A., Geurts, L., Caesar, R., et al. Intestinal epithelial MyD88 is a sensor switching host metabolism towards obesity according to nutritional status. *Nat Commun.* **5**, 5648 (2014).
10. Rutjens, E., Mazza, S., Biassoni R, Koopman G, Radic L, Fogli M, Costa P, Mingari MC, Moretta L, Heeney J, De Maria A. Differential NKp30 inducibility in chimpanzee NK cells and conserved NK cell phenotype and function in long-term HIV-1-infected animals. *J Immunol.* **178**, 1702-1712 (2007).
11. Chuang, H.C., Sheu, W.H., Lin, Y.T., et al. HGK/MAP4K4 deficiency induces TRAF2 stabilization and Th17 differentiation leading to insulin resistance. *Nat Commun.* **5**, 4602 (2014).
12. Shigeta, A., Matsumoto, M., Tedder TF, Lowe JB, Miyasaka M, Hirata T. An L-selectin ligand distinct from P-selectin glycoprotein ligand-1 is expressed on endothelial cells and promotes neutrophil rolling in inflammation. *Blood* **112**, 4915-4923 (2008).
13. Dialynas, D.P., Quan, Z.S., Wall KA, Pierres A, Quintáns J, Loken MR, Pierres M, Fitch FW. Characterization of the murine T cell surface molecule, designated L3T4, identified by monoclonal antibody GK1.5: similarity of L3T4 to the human Leu-3/T4 molecule. *J Immunol.* **131**, 2445-2451 (1983).
14. Yang, C.Y., Vogt, T.K., Favre S, Scarpellino L, Huang HY, Tacchini-Cottier F, Luther SA. Trapping of naive lymphocytes triggers rapid growth and remodeling of the fibroblast network in reactive murine lymph nodes. *Proc Natl Acad Sci U S A* **111**, 109-118 (2014).
15. Jiang, Q., Zhang, L., Wang R, Jeffrey J, Washburn ML, Brouwer D, Barbour S, Kovalev GI, Unutmaz D, Su L. FoxP3+CD4+ regulatory T cells play an important role in acute HIV-1 infection in humanized Rag2-/-gammaC-/- mice in vivo. *Blood* **112**, 2858-2868 (2008).
16. Ledbetter, J.A., Rouse, R.V., Micklem, H.S., Herzenberg LA. T cell subsets defined by expression of Lyt-1,2,3 and Thy-1 antigens. Two-parameter immunofluorescence and cytotoxicity analysis with monoclonal antibodies modifies current views. *J Exp Med.* **152**, 280-295 (1980).
17. Nakayama, K., Nakayama, K., Negishi I, Kuida K, Louie MC, Kanagawa O, Nakauchi H, Loh DY. Requirement for CD8 beta chain in positive selection of CD8-lineage T cells. *Science* **263**, 1131-1133 (1994).
18. Shih, F.F., Racz, J., Allen, P.M. Differential MHC class II presentation of a pathogenic autoantigen during health and disease. *J Immunol.* **176**, 3438-3448 (2006).
19. Wall, K.A., Lorber, M.I., Loken MR, McClatchey S, Fitch FW. Inhibition of proliferation of MIs- and Ia-reactive cloned T cells by a monoclonal antibody against a determinant shared by I-A and I-E. *J Immunol.* **131**, 1056-1064 (1983).
20. Shao, H., Peng, Y., Liao, T., Wang M, Song M, Kaplan HJ, Sun D. A shared epitope of the interphotoreceptor retinoid-binding protein recognized by the CD4+ and CD8+ autoreactive T cells. *J Immunol.* **175**, 1851-1857 (2005).
21. Charles, N., Hardwick, D., Daugas, E., Illei, G.G., Rivera, J. Basophils and the T helper 2 environment can promote the development of lupus nephritis. *Nat Med.* **16**, 701-707 (2010).
22. Doi, K., Fujimoto T, Okamura T, Ogawa M, Tanaka Y, Mototani Y, Goto M, Ota T, Matsuzaki H, Kuroki M, Tsunoda T, Sasazuki T, Shirasawa S. ZFAT plays critical roles in peripheral T cell homeostasis and its T cell receptor-mediated response. *Biochem Biophys Res Commun.* **425**, 107-112 (2012).
23. Briddell, R.A., Broudy, V.C., Bruno, E., Brandt, J.E., Srour, E.F., Hoffman, R. Further phenotypic characterization and isolation of human hematopoietic progenitor cells using a monoclonal antibody to the c-kit receptor. *Blood* **79**, 3159-3167 (1992).

24. Collins, C., Wang, J., Miao, H., Bronstein, J., Nawer H, Xu T, Figueroa M, Muntean AG, Hess JL. C/EBPα is an essential collaborator in Hoxa9/Meis1-mediated leukemogenesis. *Proc Natl Acad Sci U S A* **111**, 9899-9904 (2014).
25. Rubinstein, M.P., Kovar, M., Purton, J.F., Cho JH, Boyman O, Surh CD, Sprent J. Converting IL-15 to a superagonist by binding to soluble IL-15R{alpha}. *Proc Natl Acad Sci U S A* **103**, 9166-9171 (2006).
26. Ault, K.A., Springer, T.A. Cross-reaction of a rat-anti-mouse phagocyte-specific monoclonal antibody (anti-Mac-1) with human monocytes and natural killer cells. *J Immunol.* **126**, 359-364 (1981).
27. Lawson, B.R., Manenkova, Y., Ahamed, J., Chen, X., Zou, J.P., Baccala, R., Theofilopoulos, A.N., Yuan, C. Inhibition of transmethylation down-regulates CD4 T cell activation and curtails development of autoimmunity in a model system. *J Immunol.* **178**, 5366-5374 (2007).
28. Glass, A.M., Wolf, B.J., Schneider KM, Princiotta MF, Taffet SM. Connexin43 is dispensable for phagocytosis. *J Immunol.* **190**, 4830-4835 (2013).
29. Hasenkrug, K.J., Cory, J.M., Stimpfling, J.H. Monoclonal antibodies defining mouse tissue antigens encoded by the H-2 region. *Immunogenetics* **25**, 136-139 (1987).
30. Charles, N., Hardwick, D., Daugas, E., Illei, G.G., Rivera, J. Basophils and the T helper 2 environment can promote the development of lupus nephritis. *Nature medicine* **16**, 701-707 (2010).
31. Weng, G., Yee, F., Michl, P., Reis, D., Wahlestedt C. Studies on neuropeptide Y receptors in a mouse adrenocortical cell line. *Mol Pharmacol.* **48**, 9-14 (1995).
32. Iwamoto, S., Iwai, S., Tsujiyama K, Kurahashi C, Takeshita K, Naoe M, Masunaga A, Ogawa Y, Oguchi K, Miyazaki A. TNF-alpha drives human CD14+ monocytes to differentiate into CD70+ dendritic cells evoking Th1 and Th17 responses. *J Immunol.* **179**, 1449-1457 (2007).
33. Jutila, D.B., Kurk, S., Jutila, M.A. Differences in the expression of Ly-6C on neutrophils and monocytes following PI-PLC hydrolysis and cellular activation. *Immunol Lett.* **41**, 49-57 (1994).
34. Zuber, J., Radtke, I., Pardee, T.S., Zhao, Z., Rappaport AR, Luo W, McCurrach ME, Yang MM, Dolan ME, Kogan SC, Downing JR, Lowe SW. Mouse models of human AML accurately predict chemotherapy response. *Genes Dev.* **23**, 877-889 (2009).
35. Fujita, M., Kohanbash, G., Fellows-Mayle, W., Hamilton RL, Komohara Y, Decker SA, Ohlfest JR, Okada H. COX-2 blockade suppresses gliomagenesis by inhibiting myeloid-derived suppressor cells. *Cancer Res.* **71**, 2664-2674 (2011).
36. Kroemer, A., Xiao, X., Degauque, N., Edtinger K, Wei H, Demirci G, Li XC. The innate NK cells, allograft rejection, and a key role for IL-15. *J Immunol.* **180**, 7818-7826 (2008).
37. King, I.L., Mohrs, M. IL-4-producing CD4+ T cells in reactive lymph nodes during helminth infection are T follicular helper cells. *J Exp Med.* **206**, 1001-1007 (2009).
38. Good-Jacobson, K.L., Szumilas, C.G., Chen L, Sharpe AH, Tomayko MM, Shlomchik MJ. PD-1 regulates germinal center B cell survival and the formation and affinity of long-lived plasma cells. *Nat Immunol.* **11**, 535-542 (2010).
39. Lieberman, J. The ABCs of granule-mediated cytotoxicity: new weapons in the arsenal. *Nat Rev Immunol.* **3**, 361-370 (2003).
40. Van De Wiele, C.J., Marino JH, Murray BW, Vo SS, Whetsell ME, Teague TK. Thymocytes between the beta-selection and positive selection checkpoints are nonresponsive to IL-7 as assessed by STAT-5 phosphorylation. *J Immunol.* **172**, 4235-4244 (2004).
41. Bolotin, D.A., Mamedov, I.Z., Britanova, O.V., Zvyagin, I.V., Shagin, D., Ustyugova, S.V., Turchaninova, M.A., Lukyanov, S., Lebedev, Y.B., Chudakov, D.M. Next generation sequencing for TCR repertoire profiling: platform-specific features and correction algorithms. *Eur J Immunol.* **42**, 3073-3083 (2012).
42. Ruggiero, E., Nicolay, J.P., Fronza, R., Arens, A., Paruzynski A, Nowrouzi A, Ürenden G, Lulay C, Schneider S, Goerdt S, Glimm H, Krammer PH, Schmidt M, von

Kalle C. High-resolution analysis of the human T-cell receptor repertoire. *Nat Commun.* **6**, 8081 (2015).
43. Bolotin, D.A., Shugay, M., Mamedov, I.Z., Putintseva, E.V., Turchaninova, M.A., Zvyagin, I.V., Britanova OV, Chudakov DM. MiTCR: software for T-cell receptor sequencing data analysis. *Nature methods* **10**, 813-814 (2013).
44. Shannon, C.E. The mathematical theory of communication. 1963. *MD Comput.* **14**, 306-317 (1997).
45. Ernst, J., Kheradpour, P., Mikkelsen, T.S., Shoresh, N., Ward, L.D., et al. Mapping and analysis of chromatin state dynamics in nine human cell types. *Nature* **473**, 43-49 (2011).
46. Kundaje, A., Meuleman, W., Ernst, J., Bilenky, M., Yen, A., et al. Integrative analysis of 111 reference human epigenomes. *Nature* **518**, 317-330 (2015).
47. Schwab, L., Goroncy, L., Palaniyandi, S., Gautam, S., Triantafyllopoulou, A., Mocsai, A, Reichardt, W., Karlsson, F.J. Radhakrishnan, S.V., Hanke, K., Schmitt-Graeff, A., Freudenberg, M., von Loewenich, F.D., Wolf, P., Leonhardt, F., Baxan, N., Pfeifer, D., Schmah, O., Schönle, A., Martin, S.F., Mertelsmann, R., Duyster, J, Finke, J., Prinz, M., Henneke, P., Häcker, H., Hildebrandt, G.C., Häcker, G., Zeiser, R. Neutrophil granulocytes recruited upon translocation of intestinal bacteria enhance GvHD via tissue damage. *Nature medicine* **20**, 648-654 (2014).
48. Alpdogan, O., Eng, J.M., Muriglan, S.J., Willis, L.M., Hubbard, V.M., Tjoe, K.H., et al. Interleukin-15 enhances immune reconstitution after allogeneic bone marrow transplantation. *Blood* **105**, 865-873 (2005).
49. Tang, Z.H., et al. Tim-3/galectin-9 regulate the homeostasis of hepatic NKT cells in a murine model of nonalcoholic fatty liver disease. . *Journal of immunology* **190**, 1788-1796 (2013).
50. Palacios, R., Steinmetz, M. Il-3-dependent mouse clones that express B-220 surface antigen, contain Ig genes in germ-line configuration, and generate B lymphocytes in vivo. *Cell* **41**, 727-734 (1985).
51. Warmuth, M., Kim, S., Gu, X.J., Xia, G., Adrian, F. Ba/F3 cells and their use in kinase drug discovery. *Current opinion in oncology* **19**, 55-60 (2007).
52. Bernot, K.M., Nemer, J.S., Santhanam, R., Liu, S., Zorko, N.A., Whitman, S.P., et al. Eradicating acute myeloid leukemia in a Mll(PTD/wt):Flt3(ITD/wt) murine model: a path to novel therapeutic approaches for human disease. *Blood* **122**, 3778-3783 (2013).
53. de Both, N.J., et al. DMSO-induced terminal differentiation and trisomy 15 in myeloid cell line transformed by the Rauscher murine leukemia virus. *Cell differentiation* **10,** , 13-21 (1981).
54. Ichikawa, Y. Differentiation of a cell line of myeloid leukemia. . *Journal of cellular physiology* **74**, 223-234 (1969).
55. Warner, N.L., Moore, M.A., Metcalf, D. A transplantable myelomonocytic leukemia in BALB-c mice: cytology, karyotype, and muramidase content. *Journal of the National Cancer Institute* **43**, 963-982 (1969).
56. Matozaki, S., et al. Establishment of a myeloid leukaemic cell line (SKNO-1) from a patient with t(8;21) who acquired monosomy 17 during disease progression. *British journal of haematology* **89**, 805-811 (1995).
57. Koeffler, H.P., Golde, D.W. Acute myelogenous leukemia: a human cell line responsive to colony-stimulating activity. *Science* **200**, 1153-1154 (1978).
58. Koeffler, H.P., Billing, R., Lusis, A.J., Sparkes, R., Golde, D.W. An undifferentiated variant derived from the human acute myelogenous leukemia cell line (KG-1). *Blood* **56**, 265-273 (1980).
59. Ohyashiki, K., Ohyashiki, J.H. & Sandberg, A.A. Cytogenetic characterization of putative human myeloblastic leukemia cell lines (ML-1, -2, and -3): origin of the cells. *Cancer research* **46**, 3642-3647 (1986).

60. Gallagher, R., et al. Characterization of the continuous, differentiating myeloid cell line (HL-60) from a patient with acute promyelocytic leukemia. *Blood* **54**, 713-733 (1979).
61. Tsuchiya, S., et al. Establishment and characterization of a human acute monocytic leukemia cell line (THP-1). *Int J Cancer* **26**, 171-176 (1980).
62. Asou, H., et al. Establishment of a human acute myeloid leukemia cell line (Kasumi-1) with 8;21 chromosome translocation. *Blood* **77**, 2031-2036 (1991).
63. Lanotte, M., et al. NB4, a maturation inducible cell line with t(15;17) marker isolated from a human acute promyelocytic leukemia (M3). *Blood* **77**, 1080-1086 (1991).
64. Quentmeier, H., Reinhardt, J., Zaborski, M., Drexler, H.G. FLT3 mutations in acute myeloid leukemia cell lines. *Leukemia* **17**, 120-124 (2003).
65. Zorko, N.A., Bernot, K.M., Whitman, S.P., Siebenaler, R.F., Ahmed, E.H., Marcucci, G.G., Yanes, D.A., McConnell, K.K., Mao, C., Kalu, C., Zhang, X., Jarjoura, D., Dorrance, A.M., Heerema, N.A., Lee, B.H., Huang, G., Marcucci, G., Caligiuri, M.A. Mll partial tandem duplication and Flt3 internal tandem duplication in a double knock-in mouse recapitulates features of counterpart human acute myeloid leukemias. *Blood* **120**, 1130-1136 (2012).
66. Mizuki, M., Fenski, R., Halfter, H., et al. Flt3 mutations from patients with acute myeloid leukemia induce transformation of 32D cells mediated by the Ras and STAT5 pathways. *Blood* **96**, 3907-3914 (2000).
67. Grundler, R., Miething, C., Thiede, C., Peschel, C., Duyster, J. FLT3-ITD and tyrosine kinase domain mutants induce 2 distinct phenotypes in a murine bone marrow transplantation model. *Blood* **105**, 4792-4799 (2005).
68. Miething, C., et al. The oncogenic fusion protein nucleophosmin-anaplastic lymphoma kinase (NPM-ALK) induces two distinct malignant phenotypes in a murine retroviral transplantation model. *Oncogene* **22**, 4642-4647 (2003).
69. Saland, E., Boutzen, H., Castellano, R., et al. A robust and rapid xenograft model to assess efficacy of chemotherapeutic agents for human acute myeloid leukemia. *Blood Cancer J.* **5**, e297 (2015).
70. Zimmerman, E.I., Turner, D.C., Buaboonnam, J., Hu, S., Orwick, S., Roberts, M.S., Janke, L.J., Ramachandran, A., Stewart, C.F., Inaba, H., Baker, S.D. Crenolanib is active against models of drug-resistant FLT3-ITD-positive acute myeloid leukemia. *Blood* **122**, 3607-3615 (2013).
71. Herr, W., Eichinger, Y., Beshay, J., Bloetz, A., Vatter, S., Mirbeth, C., Distler, E., Hartwig, U.F., Thomas, S. HLA-DPB1 mismatch alleles represent powerful leukemia rejection antigens in CD4 T-cell immunotherapy after allogeneic stem-cell transplantation. . *Leukemia* **31**, 434-445 (2016).
72. Zeiser, R., Nguyen, V.H., Beilhack, A., Buess, M., Schulz, S., Baker, J., Contag, C.H., Negrin, R.S. Inhibition of CD4+CD25+ regulatory T cell function by calcineurin dependent interleukin-2 production. *Blood* **108**, 390-399 (2006).
73. Hu, S., Niu, H., Inaba, H., Orwick, S., Rose, C., Panetta, J.C., Yang, S., Pounds, S., Fan Y, Calabrese C, Rehg JE, Campana D, Rubnitz JE, Baker SD. Activity of the multikinase inhibitor sorafenib in combination with cytarabine in acute myeloid leukemia. *J Natl Cancer Inst.* **103**, 893-905 (2011).
74. Kelly, L.M., Yu, J.C., Boulton, C.L., Apatira, M., Li J, Sullivan CM, Williams I, Amaral SM, Curley DP, Duclos N, Neuberg D, Scarborough RM, Pandey A, Hollenbach S, Abe K, Lokker NA, Gilliland DG, Giese NA. CT53518, a novel selective FLT3 antagonist for the treatment of acute myelogenous leukemia (AML). *Cancer Cell* **5**, 421-432 (2002).
75. Weisberg, E., Boulton, C., Kelly, L.M., Manley, P., Fabbro, D., Meyer, T., Gilliland, D.G., Griffin, J.D. Inhibition of mutant FLT3 receptors in leukemia cells by the small molecule tyrosine kinase inhibitor PKC412. *Cancer Cell* **5**, 433-443 (2002).
76. Ma, S., Yang, L.L., Niu, T., et al. SKLB-677, an FLT3 and Wnt/β-catenin signaling inhibitor, displays potent activity in models of FLT3-driven AML. *Sci Rep.* **5**, 15646 (2015).

77. Thedieck, K., Holzwarth, B., Prentzell, M.T., et al. Inhibition of mTORC1 by astrin and stress granules prevents apoptosis in cancer cells. *Cell* **154**, 859-874 (2013).
78. Ippagunta, S.K., Malireddi, R.K., Shaw, P.J., et al. The inflammasome adaptor ASC regulates the function of adaptive immune cells by controlling Dock2-mediated Rac activation and actin polymerization. *Nat Immunol.* **12**, 1010-1016 (2011).
79. Bergstrøm, B., Aune, M.H., Awuh, J.A., et al. TLR8 Senses Staphylococcus aureus RNA in Human Primary Monocytes and Macrophages and Induces IFN-β Production via a TAK1-IKKβ-IRF5 Signaling Pathway. *J Immunol.* **195**, 1100-1111 (2015).
80. Siednienko, J., Jackson, R., Mellett, M., et al. Pellino3 targets the IRF7 pathway and facilitates autoregulation of TLR3- and viral-induced expression of type I interferons. *Nat Immunol.* **13**, 1055-1062 (2012).
81. O'Mahony, F.C., Faratian, D., Varley, J., et al. The use of automated quantitative analysis to evaluate epithelial-to-mesenchymal transition associated proteins in clear cell renal cell carcinoma. *PLoS One* **7**, e31557 (2012).
82. Le Bel, M., Gosselin, J. Leukotriene B4 Enhances NOD2-Dependent Innate Response against Influenza Virus Infection. *PLoS One* **10**, e0139856 (2015).
83. Zhang, L., Holmes, I.P,Hochgräfe, F., Walker, S.R., Ali NA, Humphrey ES, Wu J, de Silva M, Kersten WJ, Connor T, Falk H, Allan L, Street IP, Bentley JD, Pilling PA, Monahan BJ, Peat TS, Daly, R.J. Characterization of the novel broad-spectrum kinase inhibitor CTx-0294885 as an affinity reagent for mass spectrometry-based kinome profiling. *J Proteome Res.* **12**, 3104-3116 (2013).
84. Cox, J., Mann, M. MaxQuant enables high peptide identification rates, individualized p.p.b.-range mass accuracies and proteome-wide protein quantification. *Nat Biotechnol.* **12**, 1367-1372 (2008).
85. Klaeger, S., et al. Chemical Proteomics Reveals Ferrochelatase as a Common Off-target of Kinase Inhibitors. *ACS Chem Biol* **11**, 1245-1254 (2016).
86. Médard, G., et al. Optimized chemical proteomics assay for kinase inhibitor profiling. . *J Proteome Res.* **14**, 1574-1586 (2015).
87. Cox, J., Mann, M. MaxQuant enables high peptide identification rates, individualized p.p.b.-range mass accuracies and proteome-wide protein quantification. *Nat Biotechnol.* **26**, 1367-1372 (2008).
88. Cox, J., et al. Andromeda: a peptide search engine integrated into the MaxQuant environment. *J Proteome Res.* **10**, 1794-1805 (2011).
89. Cox, J., et al. Accurate proteome-wide label-free quantification by delayed normalization and maximal peptide ratio extraction, termed MaxLFQ. *Mol Cell Proteomics* **13**, 2513-2526 (2014).
90. Bantscheff, M., et al. Quantitative chemical proteomics reveals mechanisms of action of clinical ABL kinase inhibitors. *Nat Biotechnol.* **25**, 1035-1044 (2007).
91. Ritz, C., Baty, F., Streibig, J.C., Gerhard, D. Dose-Response Analysis Using R. *PLoS One* **10**, e0146021 (2015).
92. Lemeer, S., Zorgiebel, C., Ruprecht, B., Kohl, K. & Kuster, B. Comparing immobilized kinase inhibitors and covalent ATP probes for proteomic profiling of kinase expression and drug selectivity. *J Proteome Res.* **12**, 1723-1731 (2013).